

# A new species of *Nanhsiungchelys* (Testudines: Cryptodira: Nanhsiungchelyidae) from the Upper Cretaceous of Nanxiong Basin, China

Yuzheng Ke<sup>Corresp., 1</sup>, Imran A Rahman<sup>2,3</sup>, Hanchen Song<sup>1</sup>, Jinfeng Hu<sup>1</sup>, Kecheng Niu<sup>4,5</sup>, Fasheng Lou<sup>6</sup>, Hongwei Li<sup>7</sup>, Fenglu Han<sup>Corresp., 1</sup>

<sup>1</sup> School of Earth Science, China University of Geosciences (Wuhan), Wuhan, Hubei, People's Republic of China

<sup>2</sup> The Natural History Museum, London, United Kingdom

<sup>3</sup> Oxford University Museum of Natural History, Oxford, United Kingdom

<sup>4</sup> State Key Laboratory of Cellular Stress Biology, School of Life Sciences, Xiamen University, Xiamen, Fujian, People's Republic of China

<sup>5</sup> Yingliang Stone Natural History Museum, Nan'an, Fujian, People's Republic of China

<sup>6</sup> Jiangxi Geological Survey and Exploration Institute, Nanchang, Jiangxi, People's Republic of China

<sup>7</sup> Guangdong Geological Survey Institute, Guangzhou, Guangdong, People's Republic of China

Corresponding Authors: Yuzheng Ke, Fenglu Han  
Email address: key1480@163.com, hanfl@cug.edu.cn

Nanhsiungchelyidae are a group of large turtles that lived in Asia and North America during the Cretaceous. Here we report a new species of nanhsiungchelyid, *Nanhsiungchelys yangi* sp. nov., from the Upper Cretaceous of Nanxiong Basin, China. The specimen consists of a well-preserved skull and lower jaw, as well as the anterior parts of the carapace and plastron. The diagnostic features of *Nanhsiungchelys* include a large entire carapace length (~55.5 cm), a network of sculptures consisting of pits and ridges on the surface of the skull and shell, shallow cheek emargination and temporal emargination, deep nuchal emargination, and a pair of anterolateral processes on the carapace. However, *Nanhsiungchelys yangi* differs from the other species of *Nanhsiungchelys* mainly in having a triangular-shaped snout (in dorsal view) and wide anterolateral processes on the carapace. Besides, some other characteristics (e.g. the premaxilla is higher than wide, the maxilla is unseen in dorsal views, a small portion of the maxilla extends posterior and ventral of the orbit, and the parietal is bigger than the frontal) are strong evidences to distinguish *Nanhsiungchelys yangi* from *Nanhsiungchelys wuchinensis*. A phylogenetic analysis of nanhsiungchelyids places *Nanhsiungchelys yangi* and *Nanhsiungchelys wuchingensis* as sister taxa. *Nanhsiungchelys yangi* and some other nanhsiungchelyids bear distinct anterolateral processes on the carapace, which have not been reported in any extant turtles and may have played a role in protecting the head. Nanxiong Basin was extremely hot during the Late Cretaceous, and so we suggest that nanhsiungchelyids might have immersed themselves in mud or water to avoid the hot weather, similar to

some extant tortoises. If they were capable of swimming, our computer simulations of fluid flow suggest the anterolateral processes could have reduced drag during locomotion.

1  
2 **A new species of *Nanhsiungchelys* (Testudines:**  
3 **Cryptodira: Nanhsiungchelyidae) from the Upper**  
4 **Cretaceous of Nanxiong Basin, China**

5  
6  
7 Yuzheng Ke<sup>1</sup>, Imran A. Rahman<sup>2,3</sup>, Hanchen Song<sup>1</sup>, Jinfeng Hu<sup>1</sup>, Kecheng Niu<sup>4,5</sup>, Fasheng  
8 Lou<sup>6</sup>, Hongwei Li<sup>7</sup>, Fenglu Han<sup>1</sup>

9 <sup>1</sup> School of Earth Science, China University of Geosciences (Wuhan), Wuhan, Hubei, China.

10 <sup>2</sup> The Natural History Museum, London, UK.

11 <sup>3</sup> Oxford University Museum of Natural History, Oxford, UK.

12 <sup>4</sup> State Key Laboratory of Cellular Stress Biology, School of Life Sciences, Xiamen University,  
13 Xiamen, Fujian, China

14 <sup>5</sup> Yingliang Stone Natural History Museum, Nan'an, Fujian, China

15 <sup>6</sup> Jiangxi Geological Survey and Exploration Institute, Nanchang, Jiangxi, China

16 <sup>7</sup> Guangdong Geological Survey Institute, Guangzhou, Guangdong, China

17  
18 Corresponding Author:

19 Fenglu Han

20 Lumo Road, Wuhan, Hubei, 430074, China

21 Email address: hanfl@cug.edu.cn

22 Yuzheng Ke

23 Lumo Road, Wuhan, Hubei, 430074, China

24 Email address: key1480@163.com

25  
26 **Abstract**

27 Nanhsiungchelyidae are a group of large turtles that lived in Asia and North America during the  
28 Cretaceous. Here we report a new species of nanhsiungchelyid, *Nanhsiungchelys yangi* sp. nov.,  
29 from the Upper Cretaceous of Nanxiong Basin, China. The specimen consists of a well-  
30 preserved skull and lower jaw, as well as the anterior parts of the carapace and plastron. The  
31 diagnostic features of *Nanhsiungchelys* include a large entire carapace length (~55.5 cm), a  
32 network of sculptures consisting of pits and ridges on the surface of the skull and shell, shallow  
33 cheek emargination and temporal emargination, deep nuchal emargination, and a pair of  
34 anterolateral processes on the carapace. However, *Nanhsiungchelys yangi* differs from the other  
35 species of *Nanhsiungchelys* mainly in having a triangular-shaped snout (in dorsal view) and wide  
36 anterolateral processes on the carapace. Besides, some other characteristics (e.g. the premaxilla is  
37 higher than wide, the maxilla is unseen in dorsal views, a small portion of the maxilla extends  
38 posterior and ventral of the orbit, and the parietal is bigger than the frontal) are strong evidences

39 to distinguish *Nanhsiungchelys yangi* from *Nanhsiungchelys wuchingensis*. A phylogenetic  
40 analysis of nanhsiungchelyids places *Nanhsiungchelys yangi* and *Nanhsiungchelys wuchingensis*  
41 as sister taxa. *Nanhsiungchelys yangi* and some other nanhsiungchelyids bear distinct  
42 anterolateral processes on the carapace, which have not been reported in any extant turtles and  
43 may have played a role in protecting the head. Nanxiong Basin was extremely hot during the  
44 Late Cretaceous, and so we suggest that nanhsiungchelyids might have immersed themselves in  
45 mud or water to avoid the hot weather, similar to some extant tortoises. If they were capable of  
46 swimming, our computer simulations of fluid flow suggest the anterolateral processes could have  
47 reduced drag during locomotion.

48

## 49 Introduction

50 Nanhsiungchelyidae are an extinct group of Pan-Trionychia, which lived in Asia and North  
51 America from the Early Cretaceous until their extinction at the Cretaceous–Paleogene boundary  
52 (Hirayama *et al.*, 2000; Li & Tong, 2017; Joyce *et al.*, 2021). These turtles are characterized by a  
53 large body size (maximum carapace length of about 120 cm as preserved), flat carapace relative  
54 to tortoises, stubby elephantine limbs, and shells covered with a network of sculptures consisting  
55 of pits and ridges (Yeh, 1966; Hutchison & Archibald, 1986; Brinkman *et al.*, 2015; Hu *et al.*,  
56 2016; Li & Tong, 2017). In addition, these turtles produced thick-shelled (~1.8 mm) eggs and are  
57 thought to have had similar reproductive strategies to extant tortoises (e.g. large and spherical  
58 eggs) (Ke *et al.*, 2021). Recently, the morphology and phylogenetic relationships of  
59 nanhsiungchelyids have been studied in detail (Danilov *et al.*, 2013; Brinkman *et al.*, 2015; Tong  
60 *et al.*, 2016; Mallon & Brinkman, 2018; Tong & Li, 2019). Among the eight genera of  
61 Nanhsiungchelyidae, most taxa typically have a relatively short carapace, shallow nuchal  
62 emargination, narrow neurals and vertebral scutes, and lack large anterior processes on the  
63 carapace (Tong & Li, 2019). In contrast, *Nanhsiungchelys* and *Anomalocheilus* (which form a  
64 sister group) share an elongated shell, a wide and deep nuchal emargination, large anterior  
65 process on the carapace, wide neurals and vertebral scutes, and a sub-triangular first vertebral  
66 scute with a very narrow anterior end (Tong & Li, 2019). These two genera have only been found  
67 in southern China and Japan (Hirayama *et al.*, 2001; Hirayama *et al.*, 2009; Li & Tong, 2017;  
68 Tong & Li, 2019), whereas other nanhsiungchelyids have a wider geographical distribution  
69 (Danilov & Syromyatnikova, 2008; Mallon & Brinkman, 2018).

70 *Nanhsiungchelys* and *Anomalocheilus* are unique among Mesozoic turtles in possessing distinct  
71 anterolateral processes on the carapace, with a similar body structure known in the Miocene side-  
72 necked turtle *Stupendemys geographicus* (Cadena *et al.*, 2020). Palaeontologists have debated  
73 whether nanhsiungchelyids were aquatic or terrestrial for nearly 60 years (see Mallon &  
74 Brinkman (2018) for a detailed overview), but the ecological role of the anterolateral processes  
75 has largely been ignored. It was previously suggested they played a role in protecting the head  
76 (Hirayama *et al.*, 2001) or facilitating sexual displays (Hirayama & Sonoda, 2012), but further  
77 study of their function is required.

78 In China, six species of nanhsiungchelyids have been reported (Table 1), with many  
79 specimens recovered from the Upper Cretaceous of Nanxiong Basin, Guangdong Province. *Yeh*  
80 (1966) described the first species, *Nanhsiungchelys wuchingensis*, which was restudied by *Tong*  
81 & *Li* (2019). *Hirayama et al.* (2009) provided a preliminary study of a large Cretaceous turtle  
82 (SNHM 1558) which they placed within Nanhsiungchelyidae; *Li & Tong* (2017) later attributed  
83 this to *Nanhsiungchelys*. In addition, two eggs (IVPP V2789) from Nanxiong Basin were  
84 assigned to nanhsiungchelyids based on their co-occurrence with *Nanhsiungchelys wuchingensis*  
85 (*Young, 1965*).

86 Nanxiong Basin (Fig. 1A) is a NE-trending faulted basin controlled by the Nanxiong Fault in  
87 the northern margin, covering an area of about 1800 km<sup>2</sup> and spanning Guangdong and Jiangxi  
88 provinces in China (*Zhang et al., 2013*). There are well-exposed outcrops of the Cretaceous–  
89 Paleogene strata in Nanxiong Basin (*Ling et al., 2005*), and the lithostratigraphy of the Upper  
90 Cretaceous in this region has been studied extensively (see *Zhang et al. (2013)* for details). In  
91 1966, the holotype of *Nanhsiungchelys wuchingensis* (IVPP V3106) was recovered from  
92 Nanxiong Basin, with the stratum where the fossil was found named the Nanxiong Group (*Yeh*  
93 1966). Subsequently, *Zhao et al. (1991)* split Nanxiong Group into the upper Pingling Formation  
94 and lower Yuanpu Formation, reporting two K–Ar ages for the Yuanpu Formation (67.04±2.31  
95 Ma and 67.37±1.49 Ma). *Zhang et al. (2013)* further divided the original Yuanpu Formation into  
96 the Jiangtou, Yuanpu, Dafeng, and Zhutian formations, with the new Yuanpu Formation just a  
97 small part of the original Yuanpu Formation. Most recently, the Yuanpu Formation was  
98 eliminated entirely and the Nanxiong Group now consists of Dafeng, Zhutian, and Zhenshui  
99 formations (*Guangdong Geological Survey Institute, 2017*). This terminology was also used by  
100 *Xi et al. (2021)*, who summarized lithostratigraphic subdivision and correlation for the  
101 Cretaceous of China. According to this scheme, the holotype of *Nanhsiungchelys wuchingensis*  
102 (IVPP V3106) and *N. yangi* (CUGW VH108, see below) both come from the Dafeng Formation.

103 The Dafeng Formation comprises purple-red, brick-red, and brownish-red conglomerate,  
104 sandy conglomerate, and gravel-bearing sandstone, and is intercalated with sandstone, siltstone  
105 and silty mudstone (*Guangdong Geological Survey Institute, 2017*). It ranges in age from the  
106 Cenomanian to the middle Campanian (*Xi et al., 2021*). In addition to *Nanhsiungchelys*, many  
107 vertebrate fossils have been recovered from the Dafeng Formation, including: the dinosaur  
108 *Nanshiungosaurus brevispinus* (*Zanno, 2010*); the turtle eggs *Oolithes nanhsiungensis* (*Young,*  
109 *1965*); and the dinosaur eggs *Macroolithus rugustus*, *Nanhsiungoolithus chuetienensis*,  
110 *Ovaloolithus shitangensis*, *O. nanxiongensis*, and *Shixingoolithus erbeni* (*Zhao et al., 2015*).

111 Here, we report a new species of *Nanhsiungchelys* from Nanxiong Basin based on a complete  
112 skull and partial postcranial skeleton. This allows us to investigate the taxonomy and  
113 morphology of nanhsiungchelyids, and based on this we carry out a phylogenetic analysis of the  
114 group. In addition, we discuss potential functions of the large anterolateral processes (using  
115 computational fluid dynamics to test a possible role in drag reduction) and consider the  
116 implications for the ecology of this taxon.

117

## 118 **Materials & Methods**

119 **Fossil specimen.** The specimen (CUGW VH108) consists of a well-preserved skull and lower  
120 jaw, together with the anterior parts of the carapace and plastron (Figs. 2–4). This specimen was  
121 collected by a local farmer from southeast of Nanxiong Basin, near the Zhenjiang River. Based  
122 on the brownish-red siltstone near the skeleton, it was most likely from the Dafeng Formation  
123 (*Guangdong Geological Survey Institute, 2017*). CUGW VH108 is housed in the paleontological  
124 collections of China University of Geosciences (Wuhan). The skeleton was prepared using an  
125 Engraving Pen AT-310, and was photographed with a Canon EOS 6D camera.

126 **Nomenclatural acts.** The electronic version of this article in Portable Document Format (PDF)  
127 will represent a published work according to the International Commission on Zoological  
128 Nomenclature (ICZN), and hence the new names contained in the electronic version are  
129 effectively published under that Code from the electronic edition alone. This published work and  
130 the nomenclatural acts it contains have been registered in ZooBank, the online registration  
131 system for the ICZN. The ZooBank LSIDs (Life Science Identifiers) can be resolved and the  
132 associated information viewed through any standard web browser by appending the LSID to the  
133 prefix <http://zoobank.org/>. The LSID for this publication is:  
134 [urn:lsid:zoobank.org:pub:F53B5FA5-D018-453D-814D-C854810EFEFE](http://urn:lsid:zoobank.org:pub:F53B5FA5-D018-453D-814D-C854810EFEFE). The online version of  
135 this work is archived and available from the following digital repositories: PeerJ, PubMed  
136 Central SCIE and CLOCKSS.

137 **Phylogenetic analysis.** Parsimony phylogenetic analysis was performed using the software TNT  
138 1.5 (*Goloboff & Catalano, 2016*). The data matrix used herein was updated from *Tong & Li*  
139 (*2019*) and *Mallon & Brinkman (2018)*, and includes 17 taxa and 50 characters. *Adocus* was set  
140 as the outgroup following *Tong & Li (2019)*. Because there are five inframarginal scutes on  
141 *Jiangxichelys ganzhouensis* (*Tong et al., 2016*), character 37 was modified to: “Inframarginals:  
142 (0) five to three pairs; (1) two pairs; (2) absent”. In addition, character 48 was changed in  
143 *Jiangxichelys ganzhouensis* from ? to 1 (i.e. ratio of midline epiplastral suture length to total  
144 midline plastral length greater than 0.1). The length to width ratios of the carapace of  
145 *Nanhsiungchelys* and *Anomalochelys* are equal to or larger than 1.6 (*Hirayama et al., 2001*;  
146 *Hirayama et al., 2009*; *Tong & Li, 2019*), whereas the other genera (e.g. *Basilemys*) exhibit  
147 smaller ratios (*Mallon & Brinkman, 2018*). The ratio that between 1.4 and 1.6 has not been found  
148 in any nanhsiungchelyids yet. Therefore, a new character was added: “Length to width ratio of  
149 the carapace: (0) less than 1.4; (1) equal to or larger than 1.6”. Moreover, *Yuchelys nanyangensis*  
150 was added to the data matrix based on *Tong et al. (2012)*. A total of 13 characters out of 50 could  
151 be coded for *Nanhsiungchelys yangi*, representing only 26% of the total number of characters.  
152 This is because the new species is based on a partial specimen missing many of the features  
153 scored in other taxa. The analysis was conducted using a traditional search with 1000 replicates.  
154 A tree bisection reconnection (TBR) swapping algorithm was employed, and 10 trees were saved  
155 per replicate. All characters were treated as unordered and of equal weight. Standard bootstrap  
156 support values were calculated using a traditional search with 100 replicates. Bremer support  
157 values were also calculated (*Bremer, 1994*). In addition, a time-scaled phylogeny was generated

158 in R (<https://www.r-project.org/>) using our strict consensus tree and the first / last appearance  
159 datum (FAD / LAD) of all taxa. The R package Strap (*Bell & Lloyd, 2014*) was used to estimate  
160 divergence times and the function geoscalePhylo was used to plot the time-scaled tree against a  
161 geological timescale.

162 **Computational fluid dynamics.** Computational fluid dynamics (CFD) simulations of water  
163 flow were performed in the software COMSOL Multiphysics (v. 5.6). Three-dimensional digital  
164 models of *Nanhsiungchelys yangi* and two ‘hypothetical turtles’ without anterolateral processes  
165 were created using COMSOL’s in-built geometry tools. These models were placed in cylindrical  
166 flow domains, with the material properties of water assigned to the space surrounding the models  
167 and the swimming speeds of the extant large turtle used as flow velocities at the inlet. CFD  
168 simulations were performed using a stationary solver, and based on the results drag forces were  
169 extracted for each model. The main steps including the construction of digital models,  
170 specification of fluid properties and boundary conditions, meshing, and computation are detailed  
171 in Supplemental Information 3.

172 **Institutional abbreviations.** CUGW, China University of Geosciences (Wuhan), Wuhan, China;  
173 HGM, Henan Geological Museum, Zhengzhou, China; IMM, Inner Mongolia Museum, Huhhot,  
174 China; IVPP, Institute of Vertebrate Paleontology and Paleoanthropology, Chinese Academy of  
175 Sciences, Beijing, China; LJU, Lanzhou Jiaotong University, Lanzhou, China; NHMG, Natural  
176 History Museum of Guangxi, Nanning, China; NMBY, Nei Mongo Bowuguan, Huhhot, China;  
177 SNHM, Shanghai Natural History Museum, Shanghai, China; UB, University of Bristol, Bristol,  
178 UK; UPC, China University of Petroleum (East China), Qingdao, China; YSNHM, Yingliang  
179 Stone Natural History Museum, Nan’an, China.

180

## 181 **Results**

### 182 **Systematic paleontology**

183 Testudines Linnaeus, 1758

184 Cryptodira Cope, 1868

185 Nanhsiungchelyidae Yeh, 1966

186 *Nanhsiungchelys* Yeh, 1966

187 **Emended diagnosis.** A genus of Nanhsiungchelyidae of medium-large size, with an entire  
188 carapace length of 0.5–1.1 m. The surface of the skull, lower jaw, and both carapace and plastron  
189 are covered with sculptures consisting of large pits formed by a network of ridges. Temporal  
190 emargination and cheek emargination are shallow; orbits located at about mid-length of the skull  
191 and facing laterally; jugal forms the lower margin of the orbit. Carapace elongate, with a deep  
192 nuchal emargination and a pair of large anterolateral processes that extend forward and are  
193 formed entirely by the first peripheral; wide neural plates and vertebral scutes; gulars fused and  
194 extend deeply onto the entoplastron; extragulars absent; complete row of narrow inframarginals.  
195 Wide angle between the acromion process and scapula process of about 105°. One large dermal  
196 plate located above the manus.

197 **Type species.** *Nanhsiungchelys wuchingensis* Yeh, 1966

198 **Distribution.** Guangdong, China

199

200 *Nanhsiungchelys yangi* sp. nov.

201 **Etymology.** *Yangi* is in memory of paleontologist Zhongjian Yang (Chung-Chien Young).

202 **Holotype.** CUGW VH108, a partial skeleton comprising a well-preserved skull and lower jaw  
203 and the anterior parts of the carapace and plastron (Figs. 2–4).

204 **Locality and horizon.** Nanxiong, Guangdong, China. Dafeng Formation, Upper Cretaceous,  
205 Cenomanian to middle Campanian (*Xi et al., 2021*).

206 **Diagnosis.** A medium-sized species of *Nanhsiungchelys* with an estimated entire carapace length  
207 of more than 0.5 meters. It differs from *Nanhsiungchelys wuchingensis* in the following  
208 combination of characters: the snout is triangular in dorsal view; the premaxilla greater in height  
209 than length; the posteroventral ramus of the maxilla extends to the ventral region of the orbit; the  
210 dorsal margin of the maxilla is relatively straight; the jugal is greater in height than width; the  
211 prefrontal is convex dorsally behind the apertura narium externa; the temporal emargination is  
212 mainly formed by the parietal; the paired parietals are bigger than the frontals in dorsal view; the  
213 middle and posterior parts of the mandible are more robust than the most anterior part in ventral  
214 view; the anterolateral processes is wide; and the angle between the two anterior edges of the  
215 entoplastron is wide (~110°).

216 **Description.**

217 **General aspects of the skull.** The skull is large, with a length of 13 cm (Fig. 3A, B). It is well  
218 preserved but there are many cracks on its outer surface, which limit the identification of bone  
219 sutures. The snout (i.e. the parts anterior to the orbit) is large, equal to about 1/3 length of the  
220 skull, and longer than in *Jiangxichelys neimongolensis* and *Zangerlia ukhaachelys* (*Joyce &*  
221 *Norell, 2005; Brinkman et al., 2015*). In dorsal view, the snout is close to triangular in outline  
222 with a narrow anterior end (Fig. 3A, B). In lateral views, the robust snout is nearly as deep as the  
223 whole skull, with the anterior end roughly perpendicular to the horizon (Fig. 3C–F). These  
224 features differ from *Nanhsiungchelys wuchingensis* in which the snout is flattened, with the  
225 anterior end increasing in width in dorsal view (*Tong & Li, 2019*), giving it a trumpet shape. A  
226 large apertura narium externa is located in the front part of the snout, which is roughly lozenge  
227 shaped and greater in height than width in anterior view (Fig. 2). Because the posterior part of  
228 the skull is not preserved, it is difficult to accurately determine the morphological characteristics  
229 of cheek emargination (Fig. 3C–F). Nevertheless, based on the visible bone morphology, we  
230 infer that the cheek emargination was absent or low, rather than deep (i.e. to the level or even  
231 beyond the level of orbit, see e.g. *Emydura macquarrii*) (*Li & Tong, 2017*). Posteriorly, the  
232 temporal emargination is weakly developed (Fig. 3A, B), which is similar to *Nanhsiungchelys*  
233 *wuchingensis* (*Tong & Li, 2019*) and the ‘Hefei specimen’ (*Hu et al., 2016*), but differs from  
234 *Jiangxichelys neimongolensis*, *J. ganzhouensis* and *Zangerlia ukhaachelys* (*Brinkman & Peng,*  
235 *1996; Joyce & Norell, 2005; Tong et al., 2016*). The surface of the skull (as well as those of the  
236 carapace and plastron) is covered with a network of sculptures consisting of pits and ridges,  
237 which is one of the synapomorphies of Nanhsiungchelyidae (*Li & Tong, 2017*).

238 **Premaxilla.** A small bone in the anterior and ventral part of the maxilla is identified as the  
239 premaxilla (Fig. 3C–F). It is greater in height than width, similar to *Jiangxichelys*  
240 *neimongolensis* and *Zangerlia ukhaachelys* (Joyce & Norell, 2005; Brinkman et al., 2015), but  
241 differs from *Nanhsiungchelys wuchingensis* in which the premaxilla is wider than it is high in  
242 lateral view and has an inverse Y-shape in ventral view (Tong & Li, 2019). Given the existence  
243 of the large lozenge-shaped external narial opening, the contact between the left and right  
244 premaxillae may be short, unlike the condition of *Jiangxichelys neimongolensis* (Brinkman et al.,  
245 2015). However, the poor preservation of elements near the external narial opening prevents  
246 more detailed observations, and the possibility of a Y-shaped premaxilla as in *Nanhsiungchelys*  
247 *wuchingensis* cannot be excluded.

248 **Maxilla.** The maxilla is large and trapezoid in outline (Fig. 3C–F). The main body is located  
249 anterior to the orbit, but the posteroventral ramus extends to the ventral region of the orbit, which  
250 differs from the situation in *Nanhsiungchelys wuchingensis* in which the maxilla is located  
251 entirely anterior to the orbit (Tong & Li, 2019), and also differs from most other turtles  
252 (including *Zangerlia ukhaachelys* and *Jiangxichelys neimongolensis*) in which the maxilla  
253 contributes to the lower rim of the orbit (Joyce & Norell, 2005; Brinkman et al., 2015). In lateral  
254 view, the dorsal margin of the maxilla is relatively straight and extends posteriorly to the mid-  
255 region of the eye socket, which is similar to some extant turtles (e.g. *Platysternon*  
256 *megacephalum*) (Li & Tong, 2017). However, this differs from *Nanhsiungchelys wuchingensis* in  
257 which the top of the maxilla is curved dorsally (Tong & Li, 2019), and also differs from  
258 *Zangerlia ukhaachelys* and *Jiangxichelys neimongolensis* in which the top of the maxilla tapers  
259 anterodorsally (Joyce & Norell, 2005; Brinkman et al., 2015).

260 **Jugal.** The jugal is shaped like a parallelogram in lateral view (Fig. 3C–F). It is greater in height  
261 than width, unlike *Nanhsiungchelys wuchingensis* in which the jugal is wider than it is high  
262 (Tong & Li, 2019). The jugal consists of the lower rim of the orbit, which is similar to  
263 *Nanhsiungchelys wuchingensis*, but differs from most turtles in which this structure is mainly  
264 formed by the maxilla (Tong & Li, 2019). The jugal of *Nanhsiungchelys yangi* also differs from  
265 that of *Jiangxichelys ganzhouensis* in which the jugal is more posteriorly located (Tong et al.,  
266 2016). The jugal contacts with the maxilla anteriorly, and this suture is sloped. The terminal parts  
267 of the jugal contacts with the quadratojugal.

268 **Quadratojugal.** The bone that is posterior to the jugal and ventral to the postorbital is identified  
269 as the quadratojugal (Fig. 3C–F). Its location is similar in *Nanhsiungchelys wuchingensis* (Tong  
270 & Li, 2019), but the full shape is uncertain due to covering by the carapace.

271 **Prefrontal.** In dorsal view, each prefrontal is large and elongate anteroposteriorly, and narrows  
272 anteriorly and enlarges posteriorly (Fig. 3A, B). The portion in front of the orbit is entirely  
273 composed of the prefrontal (Fig. 3A, B), which differs from *Nanhsiungchelys wuchingensis* in  
274 which the maxilla extends dorsally to the prefrontal and occupies some space (Tong & Li, 2019).  
275 The paired prefrontals contact each other at the midline and form an approximate arrow shape.  
276 They form the dorsal margin of apertura narium externa anteriorly, the anterodorsal rim of the  
277 orbit posterolaterally, and contact the frontal and postorbital posteriorly (Fig. 3A, B). The contact

278 area between the prefrontal and frontal is convex anteriorly (i.e. ‘Λ’-shaped), which is similar to  
279 *Nanhsiungchelys wuchingensis* (Tong & Li, 2019). In lateral view, the prefrontal is anterior to  
280 the postorbital and dorsal to the maxilla, and consists of the anterodorsal rims of the orbit (Fig.  
281 3C–F). This is similar to *Nanhsiungchelys wuchingensis*, *Jiangxichelys neimongolensis* and  
282 *Zangerlia ukhaachelys* (Brinkman & Peng, 1996; Joyce & Norell, 2005; Tong & Li, 2019).  
283 Behind the apertura narium externa, the prefrontal is convex dorsally (Fig. 3C–F), rather than  
284 concave as in *Nanhsiungchelys wuchingensis* (Tong & Li, 2019).

285 **Frontal.** The paired frontals form a large pentagon that locate in the center of the skull roof (Fig.  
286 3A, B), which is similar to *Nanhsiungchelys wuchingensis* and *Zangerlia ukhaachelys* (Joyce &  
287 Norell, 2005; Tong & Li, 2019). Their anterior margins constitute of a “Λ” shape for articulating  
288 with the prefrontal. The lateral and posterior margins contact the postorbital and parietal  
289 respectively. The frontal is excluded from the rim of the orbit, as in *Nanhsiungchelys*  
290 *wuchingensis* and *Zangerlia ukhaachelys* (Joyce & Norell, 2005; Tong & Li, 2019). Notably,  
291 there is a line between the paired frontals (Fig. 3A, B), which might be a suture or crack. We  
292 think it most likely represents a suture since a similar structure appears in other nanhsiungchelyid  
293 specimens (Joyce & Norell, 2005; Tong & Li, 2019). Interestingly, this suture is unusually  
294 slanted, which may be the result of developmental abnormality and needs more specimens for  
295 verification.

296 **Postorbital.** The postorbital is subtriangular in outline and elongated anteroposteriorly, and it  
297 consists of part of the lateral skull roof. Most parts of the postorbital are behind the orbit, but the  
298 anterodorsal process extends to the dorsal edge of the orbit (Fig. 3C–F). Thus, the postorbital  
299 consists of the posterior-upper and posterior rims of the orbits, which is similar to  
300 *Nanhsiungchelys wuchingensis*, *Jiangxichelys ganzhouensis* and *Zangerlia ukhaachelys* (Joyce  
301 & Norell, 2005; Tong et al., 2016; Tong & Li, 2019). The postorbital contacts the prefrontal and  
302 frontal anteriorly, the jugal and quadratojugal ventrally, and the parietal medially (Fig. 3A–F). In  
303 dorsal view, the shape of the posterior margin of the postorbital is uncertain due to its poor  
304 preservation and because it is partly obscured by the carapace. It is also uncertain if the  
305 postorbital constitutes the rim of temporal emargination. Notably, the postorbital in both  
306 *Nanhsiungchelys yangi* and *N. wuchingensis* is relatively large in size (Tong & Li, 2019),  
307 whereas just a small element forms the ‘postorbital bar’ in *Jiangxichelys ganzhouensis* and  
308 *Zangerlia ukhaachelys* (Joyce & Norell, 2005; Tong et al., 2016).

309 **Parietal.** The trapezoidal parietal contributes to the posterior part of the skull roof (Fig. 3A, B),  
310 which is similar to *Nanhsiungchelys wuchingensis* (Tong & Li, 2019). However, the paired  
311 parietals are bigger than the frontals in dorsal view, contrasting with *Nanhsiungchelys*  
312 *wuchingensis* (Tong & Li, 2019). The parietal contacts the frontal anteriorly and the postorbital  
313 laterally, and these boundaries are not straight. Posteriorly, the parietal contributes to the upper  
314 temporal emarginations, but the absence of the posterior ends of the parietal (especially the right  
315 part) hampers the identification of the rim of upper temporal emarginations.

316 **Mandible.** The mandible is preserved in situ and tightly closed with the skull (Fig. 3C–F). The  
317 location of the mandible is posterior and interior to the maxillae (Fig. 4). As a result, the beak is

318 hidden, but the lower parts of the mandible can be observed. The symphysis is fused, which is  
319 similar to *Nanhsiungchelys wuchingensis* (Tong & Li, 2019). In ventral view, the most anterior  
320 part of the mandible appears slender, but the middle and posterior parts are robust (Fig. 4). This  
321 differs from *Nanhsiungchelys wuchingensis* in which nearly all parts of the mandible are equal in  
322 width (Tong & Li, 2019).

323 **Carapace.** Only the anterior parts of the carapace are preserved (Fig. 3A, B). The preserved  
324 parts indicate there is a deep nuchal emargination and a pair of anterolateral processes, which are  
325 similar to those of *Anomalochelys angulata*, *Nanhsiungchelys wuchingensis*, *Nanhsiungchelys*  
326 sp. (SNHM 1558), and the ‘Hefei specimen’ (Hirayama et al., 2001; Hirayama et al., 2009; Hu  
327 et al., 2016; Tong & Li, 2019). In contrast, the carapaces of other genera of nanhsiungchelyids  
328 (including *Basilemys*, *Hanbogdemys*, *Kharakhutulia*, *Jiangxichelys* and *Zangerlia*) usually have  
329 a shallow nuchal emargination and/or lack the distinctive anterolateral processes (Mlynarski,  
330 1972; Sukhanov, 2000; Sukhanov et al., 2008; Tong & Mo, 2010; Danilov et al., 2013; Mallon &  
331 Brinkman, 2018). In dorsal view, each anterolateral process of *Nanhsiungchelys yangi* is very  
332 wide (nearly 90°), similar to *Nanhsiungchelys wuchingensis* (Tong & Li, 2019); however, the  
333 anterolateral processes of *Anomalochelys angulata* and *Nanhsiungchelys* sp. (SNHM 1558) are  
334 slender crescent-shaped and horn-shaped, respectively, both of which are sharper than in  
335 *Nanhsiungchelys yangi* (Hirayama et al., 2001; Hirayama et al., 2009). Among the above  
336 species of *Nanhsiungchelys* and *Anomalochelys*, there is always a distinct protrusion at the tip of  
337 each anterolateral process, and this protrusion becomes more prominent in *Anomalochelys*  
338 *angulata* (Fig. 5B) and *Nanhsiungchelys* sp. (SNHM 1558) (Hirayama et al., 2001; Hirayama et  
339 al., 2009). In *Nanhsiungchelys wuchingensis* and *Anomalochelys angulata* the most anterior end  
340 of the process shows varying degrees of bifurcation (Fig. 5B) (Hirayama et al., 2001; Tong & Li,  
341 2019), but this bifurcation does not occur in *Nanhsiungchelys yangi* and *Nanhsiungchelys* sp.  
342 (SNHM 1558) (Hirayama et al., 2009). Due to the lack of sutures preserved on the surface of the  
343 carapace, it is difficult to determine whether these processes are composed of nuchal or  
344 peripheral plates. However, considering the similarity in shape of the anterolateral processes in  
345 *Nanhsiungchelys yangi* and *N. wuchingensis*, the anterolateral processes of *N. yangi* may be  
346 formed by the first peripheral plates (as in *N. wuchingensis*).

347 **Plastron.** A large plate under the mandible is identified as the anterior part of the plastron (Fig.  
348 4). The anterior edge of the epiplastron extends anteriorly beyond the deepest part of nuchal  
349 emargination (Fig. 4), similar to *Basilemys*, *Hanbogdemys*, *Jiangxichelys*, *Nanhsiungchelys*, and  
350 *Zangerlia* (Sukhanov, 2000; Danilov et al., 2013; Brinkman et al., 2015; Tong et al., 2016;  
351 Mallon & Brinkman, 2018; Tong & Li, 2019). The anterior part of the epiplastron is very thin,  
352 but it increases in thickness posteriorly and laterally (Fig. 2). Although poorly preserved, the  
353 angle between the left and right edges can be measured as about 55°, which is wider than  
354 *Hanbogdemys orientalis* (Sukhanov, 2000). The epiplastra are paired and connected at the  
355 midline. Because only the anterior part of the entoplastron is preserved, it is hard to recognize its  
356 shape. The anterior edges of the entoplastron are strongly convex, and lead into the posterior part  
357 of the epiplastra. The angle between the two anterior edges (>110°) is larger than in

358 *Nanhsiungchelys wuchingensis* (~100°) (Tong & Li, 2019). The only identifiable scutes are the  
359 gular and the humeral. In many nanhsiungchelyids, like *Basilemys praeclara*, *B. morrinensis*,  
360 *Jiangxichelys ganzhouensis*, *J. neimongolensis*, *Hanbogdemys orientalis*, *Zangerlia*  
361 *dzamynchondi* and *Kharakhutulia kalandadzei* (Brinkman & Nicholls, 1993; Brinkman & Peng,  
362 1996; Sukhanov, 2000; Sukhanov et al., 2008; Danilov et al., 2013; Tong et al., 2016; Mallon &  
363 Brinkman, 2018), there are usually extragular scutes beside the gular scutes, but this does not  
364 occur in *Nanhsiungchelys wuchingensis* (Tong & Li, 2019) and *N. yangi*. Moreover, the location  
365 and shape of the sulci of *Nanhsiungchelys yangi* are similar to *N. wuchingensis* (Tong & Li,  
366 2019). In *Nanhsiungchelys yangi*, the sulcus between the gular and humeral scutes can be  
367 identified and it is slightly curved and extend onto the entoplastron, which is similar to  
368 *Jiangxichelys neimongolensis* and *Nanhsiungchelys wuchingensis* (Brinkman & Peng, 1996;  
369 Brinkman et al., 2015; Tong & Li, 2019). However, in the other nanhsiungchelyids (e.g.  
370 *Kharakhutulia kalandadzei*, *Zangerlia dzamynchondi*, *Hanbogdemys orientalis*, *Yuchelys*  
371 *nanyangensis* and *Jiangxichelys ganzhouensis*), this sulcus is tangential to (or separated from)  
372 the entoplastron (Sukhanov, 2000; Sukhanov et al., 2008; Tong et al., 2012; Danilov et al., 2013;  
373 Tong et al., 2016).

374

## 375 Discussion

### 376 Taxonomy

377 Through comparison with a complete specimen (IVPP V3106) of *Nanhsiungchelys*  
378 *wuchingensis*, the large skull (length = 13 cm) of CUGW VH108 is inferred to correspond to an  
379 entire carapace length of ~55.5 cm (Please see Fig. 5A for a definition of ‘entire carapace  
380 length’, which comes from Hirayama et al. (2001)). This large body size, coupled with the  
381 network of sculptures on the surface of the skull and shell, clearly demonstrates that CUGW  
382 VH108 belongs to Nanhsiungchelyidae (Li & Tong, 2017). Moreover, CUGW VH108 has a  
383 laterally thickened epiplastron (Fig. 2), with the anterior edge of the epiplastron extending  
384 anterior of the deepest part of nuchal emargination (Fig. 4), additional features that are diagnostic  
385 of Nanhsiungchelyidae (Li & Tong, 2017).

386 Within Nanhsiungchelyidae, CUGW VH108 differs from *Basilemys*, *Hanbogdemys*,  
387 *Kharakhutulia*, *Yuchelys*, and *Zangerlia* because all of these taxa have weak nuchal emargination  
388 and/or lack distinct anterolateral processes (Mlynarski, 1972; Sukhanov, 2000; Sukhanov et al.,  
389 2008; Tong et al., 2012; Danilov et al., 2013; Mallon & Brinkman, 2018). Moreover, CUGW  
390 VH108 differs from *Jiangxichelys ganzhouensis* and *J. neimongolensis* in which the cheek  
391 emargination and temporal emargination are deep (Brinkman & Peng, 1996; Tong et al., 2016).  
392 Although the carapace of both *Anomalocheilus* and CUGW VH108 have deep nuchal  
393 emargination and a pair of anterolateral processes, the former’s anterolateral processes are  
394 slender crescent-shaped and have a bifurcated anterior end (Hirayama et al., 2001), which are  
395 clear differences from the wide processes of CUGW VH108.

396 CUGW VH108 is assigned to the genus *Nanhsiungchelys* based on the deep nuchal  
397 emargination, pair of anterolateral processes, and weakly developed cheek emargination and

398 temporal emargination (Li & Tong, 2017). However, CUGW VH108 differs from  
399 *Nanhsiungchelys wuchingensis* in which the snout is trumpet shaped (Tong & Li, 2019).  
400 Moreover, *Nanhsiungchelys wuchingensis* and CUGW VH108 show some differences in their  
401 skeletal features (Table 2), and in CUGW VH108 these include: the premaxilla is very small and  
402 higher than it is wide (Fig. 3C–F); the top of the maxilla is straight (in lateral views) (Fig. 3C–F);  
403 the maxilla does not occupy the space of the prefrontal (in dorsal views) (Fig. 3A, B); a small  
404 portion of the maxilla extends posterior and ventral of the orbit (Fig. 3C–F); the parallelogram  
405 jugal is greater in height than width (Fig. 3C–F); the prefrontal is convex dorsally behind the  
406 apertura narium externa; the parietals are bigger than the frontals (Fig. 3A, B); the middle and  
407 posterior parts of the mandible are more robust than the most anterior part in ventral view; and  
408 the angle between the two anterior edges of the entoplastron is wide (~110°). It is possible that  
409 the snout of the only known specimen of *Nanhsiungchelys wuchingensis* (IVPP V3106) was  
410 deformed during the burial process, as its trumpet-shaped morphology has not been reported in  
411 any other turtles. However, the post-cranial skeleton does not show much evidence of post-  
412 mortem deformation, and both Yeh (1966) and Tong & Li (2019) regarded the unique snout as an  
413 original, diagnostic characteristic. CUGW VH108 also differs from *Nanhsiungchelys* sp. (SNHM  
414 1558) in which the anterolateral processes are slender horn-shaped (Hirayama et al., 2009). The  
415 anterior processes of the ‘Hefei specimen’ are believed to be long and similar to those of  
416 *Anomalochelys angulata* (Hu et al., 2016), whereas these are relatively short in CUGW VH108.  
417 Thus, CUGW VH108 differs from all other known species of Nanhsiungchelyidae, and herein  
418 we erect the new species *Nanhsiungchelys yangi*. Lastly, on the basis of Tong & Li (2019) and  
419 our new specimen, we emended the diagnosis of *Nanhsiungchelys*. Characteristics shared by  
420 both *Nanhsiungchelys wuchingensis* and *N. yangi* are retained, and we exclude the characters  
421 that do not match *N. yangi*, such as a long and trumpet-shaped snout, large frontal, and relatively  
422 small parietal. This revised diagnosis is listed above.

423 The differences between *Nanhsiungchelys yangi* and *N. wuchingensis* are not likely to  
424 represent ontogenetic variation. Despite only corresponding to half of *Nanhsiungchelys*  
425 *wuchingensis* (IVPP V3106), the entire carapace length (~55.5 cm) of *N. yangi* (CUGW VH108)  
426 is still in the middle of the size range reported among Nanhsiungchelyidae. For instance, the  
427 entire carapace length of the Chinese nanhsiungchelyid *Jiangxichelys ganzhouensis* is ~46–74  
428 cm (Tong et al., 2016), and the estimated entire carapace length of adult nanhsiungchelyid  
429 *Kharakhutulia kalandadzei* is only ~23–25 cm (Sukhanov et al., 2008). In addition, juveniles  
430 usually have a larger skull relative to their carapace, whereas mature individuals may have a  
431 relatively smaller skull (Brinkman et al., 2013). The ratios of maximum head width (HW) to  
432 straightline carapace width (SCW) are ~30% in both *Nanhsiungchelys yangi* (CUGW VH108)  
433 and *N. wuchingensis* (IVPP V3106) (Tong & Li, 2019).

434 Sexual dimorphism is another possible explanation of the observed differences between  
435 *Nanhsiungchelys yangi* and *N. wuchingensis*, but this is very difficult to assess. Cadena et al.  
436 (2020) suggested that horns (similar to the anterolateral processes in *Nanhsiungchelys*) could be  
437 used to identify sex in the turtle *Stupendemys geographicus*. However, all known specimens of

438 *Nanhsiungchelys* exhibits distinct anterolateral processes. Some extant male tortoises (e.g.  
439 *Centrochelys sulcata*) have a more robust epiplastron than females (Zhou & Zhou, 2020), but  
440 such a difference has not been reported in *Nanhsiungchelys*. Other lines of evidence (e.g.  
441 concavity of the plastron and shape of the xiphiplastral region) commonly used to determine the  
442 sex of extant turtles (Pritchard, 2007) are also unavailable due to the poor preservation of the  
443 above specimens. Based on above discussion, the most reasonable conclusion is that CUGW  
444 VH108 represents a distinct species, rather than the product of intraspecific variation.

445

#### 446 **Phylogenetic position and paleobiogeography**

447 The phylogenetic analysis retrieved seven most parsimonious trees with a length of 77 steps,  
448 with a consistency index (CI) of 0.675 and retention index (RI) of 0.679. The strict consensus  
449 tree (Fig. 6) recovers *Nanhsiungchelys yangi* and *N. wuchingensis* as sister taxa, with one  
450 unambiguous synapomorphy identified: the absence of the extragulars. These two species and  
451 *Anomalochelys angulata* form a monophyletic group, which is consistent with the results of Tong  
452 & Li (2019). Synapomorphies of this group include wide neurals, first vertebral scute with lateral  
453 edges converging anteriorly, cervical scute as wide as long, and the length to width ratio of the  
454 carapace is larger than 1.6. In particular, our new character (character 50, the length to width  
455 ratio of the carapace) supports this relationship, suggesting it could prove informative in other  
456 studies of turtle phylogeny. However, the standard bootstrap and Bremer supports values are low  
457 among these groups, and their relationships therefore need further consideration. Interestingly,  
458 our new results identify *Yuchelys nanyangensis* and *Zangerlia testudinimorpha* as sister taxa, and  
459 this relationship was supported by one unambiguous synapomorphy (their fifth vertebral almost  
460 fully covers the suprapygal). However, this relationship needs to be tested in future work as the  
461 only known specimen of *Yuchelys nanyangensis* (HGM NR09-11-14) is poorly preserved (Tong  
462 *et al.*, 2012) and only 15 characters could be used in our phylogenetic analysis.

463 Although *Anomalochelys* and *Nanhsiungchelys* were in similar stages (Fig. 6), they appear to  
464 have lived in different regions (southern China and Japan, respectively). In fact, Cretaceous turtle  
465 communities in Japan and the rest of Asia (especially China and Mongolia) are closely  
466 comparable, with both areas containing representatives of Adocusia, Lindholmemydidae,  
467 Sinochelyidae, and Sinemydidae (Hirayama *et al.*, 2000). Similar extinct organisms in these  
468 regions also include the plant *Neozamites* (Sun *et al.*, 1993; Duan, 2005), the bivalve  
469 *Trigonioides* (Ma, 1994; Komatsu *et al.*, 2007), and the dinosaur Hadrosaurinae (Kobayashi *et*  
470 *al.*, 2019; Zhang *et al.*, 2020). Sun & Yang (2010) inferred that the Japan Sea did not exist during  
471 the Jurassic and Cretaceous, with the Japan archipelago still closely linked to the eastern  
472 continental margin of East Asia. This view is also supported by geological and geophysical  
473 evidence (Kaneoka *et al.*, 1990; Liu *et al.*, 2017). In addition to *Anomalochelys angulata* from  
474 Hokkaido (Hirayama *et al.*, 2001), many fragments of Nanhsiungchelyidae (as *Basilemys* sp.)  
475 have also been found on Honshu and Kyushu islands, Japan (Hirayama, 1998; Hirayama, 2002;  
476 Danilov & Syromyatnikova, 2008). In China, the easternmost specimen of a nanhsiungchelyid  
477 turtle (a fragment of the shell) was recovered from the Upper Cretaceous of Laiyang, Shandong

478 (*Li & Tong, 2017*), which is near the west coast of the Pacific Ocean and close to Japan  
479 geographically. This geographical proximity likely allowed nanhsiungchelyids to migrate  
480 between China and Japan during the Late Cretaceous.

481

#### 482 **Function of the anterolateral processes of the carapace**

483 The anterolateral processes of *Nanhsiungchelys* (and *Anomalochelys*) have performed a  
484 variety of functions, but the principal function was most likely self-protection. In the earliest  
485 research on *Nanhsiungchelys wuchingensis*, *Yeh (1966)* did not discuss the function of the  
486 anterolateral processes, but speculated that the neck was flexible and the skull could be  
487 withdrawn into the shell to avoid danger. This hypothesis was supported by a complete specimen  
488 (93NMBY-2) of nanhsiungchelyid *Jiangxichelys neimongolensis* whose head was withdrawn  
489 into the shell (*Brinkman et al., 2015*). In contrast, *Hirayama et al. (2001)* suggested that the large  
490 skull could not be fully withdrawn within the shell (parallel to the extant big-headed turtle  
491 *Platysternon megacephalum*) and the anterolateral processes of *Nanhsiungchelys wuchingensis*  
492 and *Anomalochelys angulata* were used for protecting the skull. *Hirayama et al. (2001)* also  
493 noted that *Nanhsiungchelys* has undeveloped temporal emargination, whereas *Jiangxichelys* has  
494 distinct temporal emargination, and the former condition could inhibit the ability to retract the  
495 skull inside the shell (*Hirayama et al., 2009; Werneburg, 2015; Hermanson et al., 2022*).  
496 Together, this suggests that despite the possession of a flexible neck that could have made it  
497 possible to retract the head, the large size of the skull and the reduced temporal emargination  
498 were considerable obstacles to doing so. Today, turtles that cannot retract the head are restricted  
499 to a few aquatic groups (e.g. *Platysternidae*) (*Zhou & Li, 2013*), whereas most turtles (including  
500 all tortoises) have this capability (*Zhou & Zhou, 2020*). Additional strong piece of evidence that  
501 *Nanhsiungchelys* could not retract the head is that the skulls of all known specimens (IVPP  
502 V3106, SNHM 1558, and CUGW VH108) are preserved outside of the shell, and the  
503 anterolateral processes would thus provide lateral protection for the head (*Yeh, 1966; Hirayama*  
504 *et al., 2009; Tong & Li, 2019*). Nevertheless, it seems evident that this protective strategy of  
505 *Nanhsiungchelys* was inefficient as the dorsal side of the head would be left vulnerable to attack,  
506 and this may explain why extant terrestrial turtles usually abandon this mode of protection.

507 The anterolateral processes might also have been used during fighting for mates, as  
508 hypothesized for the extinct side-necked turtle *Stupendemys geographicus* (*Cadena et al., 2020*).  
509 Nanhsiungchelyids and extant tortoises share many comparable skeletal characteristics  
510 (*Hutchison & Archibald, 1986*) and inferred reproductive behaviors (*Ke et al., 2021*), and thus  
511 *Nanhsiungchelys* might have been characterized by similar combat behavior. A parallel  
512 hypothesis was proposed by *Hirayama & Sonoda (2012)* that the combinations of cranial and  
513 nuchal morphology in *Nanhsiungchelys* and *Anomalochelys* could facilitate sexual displays,  
514 similar to some extant testudinids. However, all known specimens of *Nanhsiungchelys* and  
515 *Anomalochelys* possess distinct anterolateral processes and deep nuchal emargination, suggesting  
516 these structures might also have been present in females (although this is uncertain because it is  
517 not possible to determine their sex). If so, the anterolateral processes would not be the result of

518 sexual dimorphism and associated combat or display. Another piece of evidence arguing against  
519 the fighting view is that there are no scars on the anterolateral processes of CUGW VH108, as  
520 might be expected if they were used in fighting.

521 The anterolateral processes of *Nanhsiungchelys* might also have had a secondary function in  
522 reducing drag as the animal was moving through water. Today, some tortoises living in dry areas  
523 (e.g. *Aldabrachelys gigantea* and *Centrochelys sulcata*) will immerse themselves in mud or  
524 water for a long time to avoid the hot weather (Zhou & Zhou, 2020), and *Aldabrachelys gigantea*  
525 could even swim (or float) in the ocean (Gerlach et al., 2006; Hansen et al., 2016). Nanxiong  
526 Basin was extremely hot (~27–34 °C) during the Late Cretaceous (Yang et al., 1993), and the  
527 appearance of diverse fossils of Gastropoda, Bivalvia, Charophyceae, and Ostracoda (Zhang et  
528 al., 2013) suggests the existence of lakes or rivers. Thus, *Nanhsiungchelys* may have had a  
529 parallel lifestyle to these tortoises, and the reduction of drag could have been important under  
530 these circumstances. Nesson (1984) also mentioned nanhsiungchelyids would anchor themselves  
531 on the bottom of streams to offset drift, which could be an adaptation to strong currents. The  
532 anterolateral processes of *Nanhsiungchelys* could have played a role in reducing resistance to  
533 fluid motion, and the efficiency of this would have been close to the level of extant freshwater  
534 turtles (see Supplemental Information 3 for detailed information on hydrodynamic analyses). The  
535 reason for this is that these processes made the anterior part of the shell more streamlined (Fig.  
536 7A, B), analogous to the streamlined fairing on the anterior of airplanes and rockets. However,  
537 we acknowledge this remains a hypothesis at this time, since there is no conclusive evidence of  
538 swimming in *Nanhsiungchelys*.

539 Many of the specialized morphological features of nanhsiungchelyids (e.g. huge skull, distinct  
540 anterolateral processes, and unusually thick eggshells) are most likely adaptations to their  
541 environment. *Nanhsiungchelys* was a successful genus since it belongs to the only group of  
542 turtles that has been reported from the Dafeng Formation, suggesting these unusual turtles were  
543 well adapted to their environment. However, their specialist survival strategies might have been  
544 very inefficient because the anterolateral processes could not protect the dorsal side of the head,  
545 and the thick eggshell (Ke et al., 2021) might have hindered the breathing and hatching of young.  
546 All of these features are not present in extant turtles, suggesting this was not a dominant  
547 direction in turtle evolution. Consistent with this, nanhsiungchelyids became extinct at the end of  
548 the Cretaceous, but many contemporary turtles (e.g. Adocidae, Lindholmemydidae, and  
549 Trionychidae) survived into the Cenozoic (Lichtig & Lucas, 2016).

550

## 551 Conclusions

552 A turtle skeleton (CUGW VH108) with a well-preserved skull and lower jaw, together with  
553 the anterior parts of the shell, was found in Nanxiong Basin, China. This is assigned to the genus  
554 *Nanhsiungchelys* based on the large estimated body size (~55.5 cm), the presence of a network  
555 of sculptures on the surface of the skull and shell, shallow cheek emargination and temporal  
556 emargination, deep nuchal emargination, and a pair of anterolateral processes on the carapace.  
557 Based on the character combination of a triangular-shaped snout (in dorsal view) and wide

558 anterolateral processes, we erect a new species *Nanhsiungchelys yangi*. A phylogenetic analysis  
559 of nanhsiungchelyids places *Nanhsiungchelys yangi* and *N. wuchingensis* as sister taxa. We agree  
560 with previous suggestions that the anterolateral processes on the carapace could have protected  
561 the head, but also infer a potential secondary function for reducing drag force during movement  
562 through water. These unique characteristics might have helped nanhsiungchelyids survive in a  
563 harsh environment, but did not save them from extinction during the K-Pg event.

564

## 565 Acknowledgements

566 We thank Xing Xu (IVPP) for his useful suggestions, thank Kaifeng Wu (YSNHM) for  
567 preparing turtle skeleton, and thank Mingbo Wang (UPC), Zichuan Qin (UB), Wen Deng  
568 (CUGW) and Haoran Sun (LJU) for assistance with CFD.

569

## 570 References

- 571 **Bell MA, Lloyd GT. 2014.** strap: an R package for plotting phylogenies against stratigraphy and  
572 assessing their stratigraphic congruence. *Palaeontology* **58**:379-389. DOI:10.1111/pala.12142
- 573 **Bremer K. 1994.** Branch support and tree stability. *Cladistics* **10**:295-304. DOI:10.1111/j.1096-  
574 0031.1994.tb00179.x
- 575 **Brinkman D, Nicholls EL. 1993.** New specimen of *Basilemys praeclara* Hay and its bearing on  
576 the relationships of the Nanhsiungchelyidae (Reptilia: Testudines). *Journal of Paleontology*  
577 **67**:1027-1031. DOI:10.1017/s002233600002535x
- 578 **Brinkman D, Peng J-H. 1996.** A new species of *Zangerlia* (Testudines: Nanhsiungchelyidae)  
579 from the Upper Cretaceous redbeds at Bayan Mandahu, Inner Mongolia, and the relationships  
580 of the genus. *Canadian Journal of Earth Sciences* **33**:526-540. DOI:10.1139/e96-041
- 581 **Brinkman DB, Tong H-Y, Li H, Sun Y, Zhang J-S, Godefroit P, Zhang Z-M. 2015.** New  
582 exceptionally well-preserved specimens of “*Zangerlia*” *neimongolensis* from Bayan Mandahu,  
583 Inner Mongolia, and their taxonomic significance. *Comptes Rendus Palevol* **14**:577-587.  
584 DOI:10.1016/j.crpv.2014.12.005
- 585 **Brinkman DB, Yuan C-X, Ji Q, Li D-Q, You H-L. 2013.** A new turtle from the Xiagou  
586 Formation (Early Cretaceous) of Changma Basin, Gansu Province, P. R. China.  
587 *Palaeobiodiversity and Palaeoenvironments* **93**:367-382. DOI:10.1007/s12549-013-0113-0
- 588 **Bureau of Geology and Mineral Exploration and Development of Jiangxi Province. 2017.**  
589 *Regional geology of China, Jiangxi Province*. Beijing: Geological Publishing House. (in  
590 Chinese with English abstract)
- 591 **Cadena E-A, Scheyer TM, Carrillo-Briceño JD, Sánchez R, Aguilera-Socorro OA, Vanegas  
592 A, Pardo M, Hansen DM, Sánchez-Villagra MR. 2020.** The anatomy, paleobiology, and  
593 evolutionary relationships of the largest extinct side-necked turtle. *Science Advances*  
594 **6**:eaay4593. DOI:10.1126/sciadv.aay4593
- 595 **Danilov IG, Sukhanov VB, Syromyatnikova EV. 2013.** Redescription of *Zangerlia*  
596 *dzamynchondi* (Testudines: Nanhsiungchelyidae) from the Late Cretaceous of Mongolia, with  
597 a reassessment of the phylogenetic position and relationships of *Zangerlia*. *Morphology and*

- 598 *Evolution of Turtles*, 407-417.
- 599 **Danilov IG, Syromyatnikova EV. 2008.** New materials on turtles of the family  
600 Nanhsiungchelyidae from the Cretaceous of Uzbekistan and Mongolia, with a review of the  
601 nanhsiungchelyid record in Asia. *Proceedings of the Zoological Institute RAS* **312**:3-25.
- 602 **Duan Y. 2005.** A new material of *Neozamites* from Yixian Formation of western Liaoning and  
603 its paleophytogeographic significance. *Global Geology* **24**:112-116. (in Chinese with English  
604 abstract)
- 605 **Gerlach J, Muir C, Richmond MD. 2006.** The first substantiated case of trans-oceanic tortoise  
606 dispersal. *Journal of Natural History* **40**:2403-2408. DOI:10.1080/00222930601058290
- 607 **Goloboff PA, Catalano SA. 2016.** TNT version 1.5, including a full implementation of  
608 phylogenetic morphometrics. *Cladistics* **32**:221-238. DOI: 10.1111/cla.12160
- 609 **Guangdong Geological Survey Institute. 2017.** *Regional geology of Guangdong, Xianggang,  
610 and Aomen (second edition)*. (in Chinese)
- 611 **Hansen DM, Austin JJ, Baxter RH, Boer EJD, Falcón W, Norder SJ, Rijdsdijk KF, Thébaud  
612 C, Bunbury NJ, Warren BH. 2016.** Origins of endemic island tortoises in the western Indian  
613 Ocean: a critique of the human-translocation hypothesis. *Journal of Biogeography* **44**:1430–  
614 1435. DOI:10.1111/jbi.12893
- 615 **Hermanson G, Benson RBJ, Farina BM, Ferreira GS, Langer MC, Evers SW. 2022.** Cranial  
616 ecomorphology of turtles and neck retraction as a possible trigger of ecological diversification.  
617 *Evolution*:1-21. DOI: 10.1111/evo.14629
- 618 **Hirayama R. 1998.** Fossil turtles from the Mifune Group (Late Cretaceous) of Kumamoto  
619 Prefecture, Western Japan. Report of the research on the distribution of important fossils in  
620 Kumamoto Prefecture: Dinosaurs from the Mifune Group, Kumamoto Prefecture, Japan: 85-  
621 99. (in Japanese with English abstract)
- 622 **Hirayama R. 2002.** Preliminary report of the fossil turtles from the Kitadani Formation (Early  
623 Cretaceous) of the Tetori Group of Katsuyama, Fukui Prefecture, Central Japan. *Memoir of the  
624 Fukui Prefectural Dinosaur Museum* **1**:29-40. (in Japanese with English abstract)
- 625 **Hirayama R, Brinkman DB, Danilov IG. 2000.** Distribution and biogeography of non-marine  
626 Cretaceous turtles. *Russian Journal of Herpetology* **7**:181–198.
- 627 **Hirayama R, Sakurai K, Chitoku T, Kawakami G, Kito N. 2001.** *Anomalocheilus angulata*,  
628 an unusual land turtle of family Nanhsiungchelyidae (superfamily Trionychoidea; order  
629 Testudines) from the Upper Cretaceous of Hokkaido, North Japan. *Russian Journal of  
630 Herpetology* **8**:127-138.
- 631 **Hirayama R, Sonoda T. 2012.** Morphology and evolution of Nanhsiungchelyidae (Cryptodira:  
632 Trionychia). [Abstract] *Symposium on Turtle Evolution*: 21.
- 633 **Hirayama R, Zhong Y, Di Y, Yonezawa T, Hasegawa M. 2009.** A new nanhsiungchelyid  
634 turtle from Late Cretaceous of Guangdong, China. In: Brinkman D, ed. *Gaffney Turtle  
635 Symposium*: Drumheller: Royal Tyrell Museum, 72-73.
- 636 **Hu Y, Huang J, Obratzsova EM, Syromyatnikova EV, Danilov IG. 2016.** A new  
637 nanhsiungchelyid turtle from the Late Cretaceous of Jiangxi, China. [Abstract] *SVP 76th*

- 638 *Annual meeting*: 158.
- 639 **Hutchison JH, Archibald JD. 1986.** Diversity of turtles across the Cretaceous/Tertiary  
640 boundary in northeastern Montana. *Palaeogeography, Palaeoclimatology, Palaeoecology*  
641 **55**:1-22. DOI:10.1016/0031-0182(86)90133-1
- 642 **Jerzykiewicz T, Currie PJ, Eberth DA, Johnsto PA, Koster EH, Zheng J-J. 1993.** Djadokhta  
643 Formation correlative strata in Chinese Inner Mongolia: an overview of the stratigraphy,  
644 sedimentary geology, and paleontology and comparisons with the type locality in the pre-Altai  
645 Gobi. *Canadian Journal of Earth Science* **30**:2180-2195. DOI:10.1139/e93-190
- 646 **Joyce WG, Anquetin J, Cadena E-A, Claude J, Danilov IG, Evers SW, Ferreira GS, Gentry**  
647 **AD, Georgalis GL, Lyson TR, Pérez-García A, Rabi M, Sterli J, Vitek NS, Parham JF.**  
648 **2021.** A nomenclature for fossil and living turtles using phylogenetically defined clade names.  
649 *Swiss Journal of Palaeontology* **140**:1-45. DOI:10.1186/s13358-020-00211-x
- 650 **Joyce WG, Norell MA. 2005.** *Zangerlia ukhaachelys*, new species, a nanhsiungchelyid turtle  
651 from the Late Cretaceous of Ukhaa Tolgod, Mongolia. *American Museum Novitates* **3481**:1-  
652 20. DOI:10.1206/0003-0082(2005)481[0001:Zunsan]2.0.Co;2
- 653 **Kaneoka I, Notsu K, Takigami Y, Fujioka K, Sakai H. 1990.** Constraints on the evolution of  
654 the Japan Sea based on <sup>40</sup>Ar-<sup>39</sup>Ar ages and Sr isotopic ratios for volcanic rocks of the Yamato  
655 Seamount chain in the Japan Sea. *Earth and Planetary Science Letters* **97**:211-225.  
656 DOI:10.1016/0012-821x(90)90109-b
- 657 **Ke Y, Wu R, Zelenitsky DK, Brinkman D, Hu J, Zhang S, Jiang H, Han F. 2021.** A large  
658 and unusually thick-shelled turtle egg with embryonic remains from the Upper Cretaceous of  
659 China. *Proceedings of the Royal Society B-Biological Sciences* **288**:20211239.  
660 DOI:10.1098/rspb.2021.1239
- 661 **Kobayashi Y, Nishimura T, Takasaki R, Chiba K, Fiorillo AR, Tanaka K, Chinzorig T,**  
662 **Sato T, Sakurai K. 2019.** A new hadrosaurine (Dinosauria: Hadrosauridae) from the marine  
663 deposits of the Late Cretaceous Hakobuchi Formation, Yezo Group, Japan. *Scientific reports*  
664 **9**:1-14. DOI:10.1038/s41598-019-48607-1
- 665 **Komatsu T, Jinhua C, Ugai H, Hirose K. 2007.** Notes on non-marine bivalve *Trigonioides*  
666 (*Trigonioides*?) from the mid-Cretaceous Goshoura Group, Kyushu, Japan. *Journal of Asian*  
667 *Earth Sciences* **29**:795–802. DOI:10.1016/j.jseas.2006.06.001
- 668 **Li J, Tong H. 2017.** *Palaeovertebrata sinica, volume II, amphibians, reptilians, and avians,*  
669 *fascicle 2 (serial no. 6), parareptilians, captorhines, and testudines.* Beijing: Science Press. (in  
670 Chinese)
- 671 **Lichtig AJ, Lucas SG. 2016.** Cretaceous nonmarine turtle biostratigraphy and evolutionary  
672 events. *Cretaceous Period: Biotic Diversity and Biogeography New Mexico Museum of*  
673 *Natural History and Science Bulletin* **71**:185-194.
- 674 **Ling Q, Zhang X, Lin J. 2005.** New advance in the study of the Cretaceous and Paleogene  
675 strata of the Nanxiong Basin. *Journal of Stratigraphy* **29**:596-601. (in Chinese with English  
676 abstract)
- 677 **Liu M, Wei D, Shi Y. 2017.** Review on the opening and evolution models of the Japan sea.

- 678 *Progress in Geophysics* **32**:2341-2352. (in Chinese with English abstract)
- 679 **Ma Q.** 1994. Nonmarine Cretaceous bivalve assemblages in China. *Cretaceous Research*
- 680 **15**:271-284. DOI:10.1006/cres.1994.1017
- 681 **Mallon JC, Brinkman DB.** 2018. *Basilemys morrinensis*, a new species of nanhsiungchelyid
- 682 turtle from the Horseshoe Canyon Formation (Upper Cretaceous) of Alberta, Canada. *Journal*
- 683 *of Vertebrate Paleontology* **38**:e1431922. DOI:10.1080/02724634.2018.1431922
- 684 **Mlynarski M.** 1972. *Zangerlia testudinimorpha* n. gen., n. sp., a primitive land tortoise from the
- 685 Upper Cretaceous of Mongolia. *Palaeontologia Polonica* **27**:85-92.
- 686 **Nessov LA.** 1984. Data on Late Mesozoic turtles from the USSR. *Studia Geologica*
- 687 *Salmanticensia especial* **1**:215-233.
- 688 **Pritchard PCH.** 2007. Evolution and structure of the turtle shell. In: Wyneken J, Godfrey MH,
- 689 and Bels V, eds. *Biology of turtles*. Boca Raton, FL: CRC Press, 45-84.
- 690 **Sukhanov VB.** 2000. Mesozoic turtles of Middle and Central Asia. In: Benton MJ, Shishkin MA,
- 691 Unwin DM, and Kurochkin EN, eds. *The age of dinosaurs in Russia and Mongolia*.
- 692 Cambridge: Cambridge University Press, 309-367.
- 693 **Sukhanov VB, Danilov IG, and Syromyatnikova EV.** 2008. The description and phylogenetic
- 694 position of a new nanhsiungchelyid turtle from the Late Cretaceous of Mongolia. *Acta*
- 695 *Palaeontologica Polonica* **53**:601-614. DOI:10.4202/app.2008.0405
- 696 **Sun G, Nakazawa T, Ohana T, Kimura T.** 1993. Two *Neozamites* species (Bennettitales) from
- 697 the Lower Cretaceous of Northeast China and the inner zone of Japan. *Transactions and*
- 698 *proceedings of the Paleontological Society of Japan New series* **172**:264-276.
- 699 **Sun G, Yang T.** 2010. Paleontological evidence-based discussion on the origin of the Japan Sea.
- 700 *Marine Sciences* **34**:89-92. (in Chinese)
- 701 **Syromyatnikova EV, Danilov IG.** 2009. New material and a revision of turtles of the genus
- 702 *Adocus* (Adocidae) from the Late Cretaceous of middle Asia and Kazakhstan. *Proceedings of*
- 703 *the Zoological Institute RAS* **313**:74-94.
- 704 **Tong H, Li L.** 2019. A revision of the holotype of *Nanhsiungchelys wuchingensis*, Ye, 1966
- 705 (Testudines: Cryptodira: Trionychoidea: Nanhsiungchelyidae). *Cretaceous Research* **95**:151-
- 706 163. DOI:10.1016/j.cretres.2018.11.003
- 707 **Tong H, Li L, Jie C, Yi L.** 2016. New material of *Jiangxichelys ganzhouensis* Tong & Mo,
- 708 2010 (Testudines: Cryptodira: Nanhsiungchelyidae) and its phylogenetic and
- 709 palaeogeographical implications. *Geological Magazine* **154**:456-464.
- 710 DOI:10.1017/s0016756816000108
- 711 **Tong H, Mo J.** 2010. *Jiangxichelys*, a new nanhsiungchelyid turtle from the Late Cretaceous of
- 712 Ganzhou, Jiangxi Province, China. *Geological Magazine* **147**:981-986.
- 713 DOI:10.1017/s0016756810000671
- 714 **Tong H, Xu L, Buffetaut E, Zhang X, Jia S.** 2012. A new nanhsiungchelyid turtle from the
- 715 Late Cretaceous of Neixiang, Henan Province, China. *Annales de Paléontologie* **98**:303-314.
- 716 DOI:10.1016/j.annpal.2012.08.001
- 717 **Wang W, Liu X, Ma M, Mao X, Ji J.** 2016. Sedimentary environment of Cretaceous red beds

- 718 in Nanxiong Basin, Guangdong Province. *Journal of Subtropical Resources and Environment*  
719 **11**:29-37. (in Chinese with English abstract)
- 720 **Wang Y, Li Q, Bai B, Jin X, Mao F, Meng J. 2019.** Paleogene integrative stratigraphy and  
721 timescale of China. *Science China Earth Sciences* **49**:289–314. (in Chinese)
- 722 **Werneburg I. 2015.** Neck motion in turtles and its relation to the shape of the temporal skull  
723 region. *Comptes Rendus Palevol* **14**:527-548. DOI:10.1016/j.crpv.2015.01.007
- 724 **Xi D, Sun L, Qin Z, Li G, Li G, Wan X. 2021.** Lithostratigraphic subdivision and correlation of  
725 the Cretaceous in China. *Journal of Stratigraphy* **45**:375-401. (in Chinese with English  
726 abstract)
- 727 **Xu X, Pittman M, Sullivan C, Choiniere JN, Tan Q-W, Clark JM, Norell MA, Wang S.**  
728 **2015.** The taxonomic status of the Late Cretaceous dromaeosaurid *Linheraptor exquisitus* and  
729 its implications for dromaeosaurid systematics. *Vertebrata Palasiatica* **53**:29-62.
- 730 **Yang W, Chen N, Ni S, Nan J, Wu M, Jiang J, Ye J, Feng X, Ran Y. 1993.** Carbon and  
731 oxygen isotopic composition and environmental significance of Cretaceous red-bed carbonate  
732 rocks and dinosaur eggshells. *Chinese Science Bulletin* **38**:2161-2163. (in Chinese)
- 733 **Yeh H-K. 1966.** A new Cretaceous turtle of Nanhsiung, Northern Kwangtung. *Vertebrata*  
734 *Palasiatica* **10**:191-200.
- 735 **Young C-C. 1965.** Fossil eggs from Nanhsiung, Kwangtung and Kanchou, Kiangsi. *Vertebrata*  
736 *Palasiatica* **9**:141-159. (in Chinese with English abstract)
- 737 **Zanno LE. 2010.** A taxonomic and phylogenetic re-evaluation of Therizinosauria (Dinosauria:  
738 Maniraptora). *Journal of Systematic Palaeontology* **8**:503–543.  
739 DOI:10.1080/14772019.2010.488045
- 740 **Zhang X-q, Zhang X-m, Hou M-c, Li G, Li H-m. 2013.** Lithostratigraphic subdivision of red  
741 beds in Nanxiong Basin, Guangdong, China. *Journal of Stratigraphy* **37**:441-451. (in Chinese  
742 with English abstract)
- 743 **Zhang Y-G, Wang K-B, Chen S-Q, Liu D, Xing H. 2020.** Osteological re-assessment and  
744 taxonomic revision of “*Tanius laiyangensis*” (Ornithischia: Hadrosauroidea) from the Upper  
745 Cretaceous of Shandong, China. *The Anatomical Record* **303**:790-800.  
746 DOI:10.1002/AR.24097
- 747 **Zhao Z, Wang Q, Zhang S. 2015.** *Palaeovertebrata Sinica, Volume II, Amphibians, Reptilians,*  
748 *and Avians, Fascicle 7 (Serial no.11), Dinosaur Eggs.* Beijing: Science Press. (in Chinese)
- 749 **Zhao Z, Ye J, Li H, Zhao Z, Yan Z. 1991.** Extinction of dinosaurs at Cretaceous-Tertiary  
750 boundary in Nanxiong Basin, Guangdong Province. *Vertebrata Palasiatica* **29**:1-12. (in  
751 Chinese)
- 752 **Zhou T, Li P. 2013.** *Primary color illustrated handbook of classification of Chinese turtles.*  
753 Beijing: China Agriculture Press. (in Chinese)
- 754 **Zhou T, Zhou F. 2020.** *Tortoises of the World.* Beijing: China Agriculture Press. (in Chinese)
- 755

## Figure 1

Geological map of Nanxiong Basin and stratigraphic distribution of valid nanhsiungchelyid turtles in China.

(A) Geological map of Nanxiong Basin, and the red triangular indicates fossil site, after Wang et al. (2016), Wang et al. (2019) and Xi et al. (2021). (B) Stratigraphic distribution of valid nanhsiungchelyid turtles in China. Abbreviations: Cam, Campanian; Cen, Cenomanian; Con, Coniacian; Maa, Maastrichtian; San, Santonian; Tur, Turonian. Stratigraphic information based on work by the Bureau of Geology and Mineral Exploration and Development of Jiangxi Province (2017) , Guangdong Geological Survey Institute (2017) , Jerzykiewicz et al. (1993) , Xi et al. (2021) , and Xu et al. (2015) .

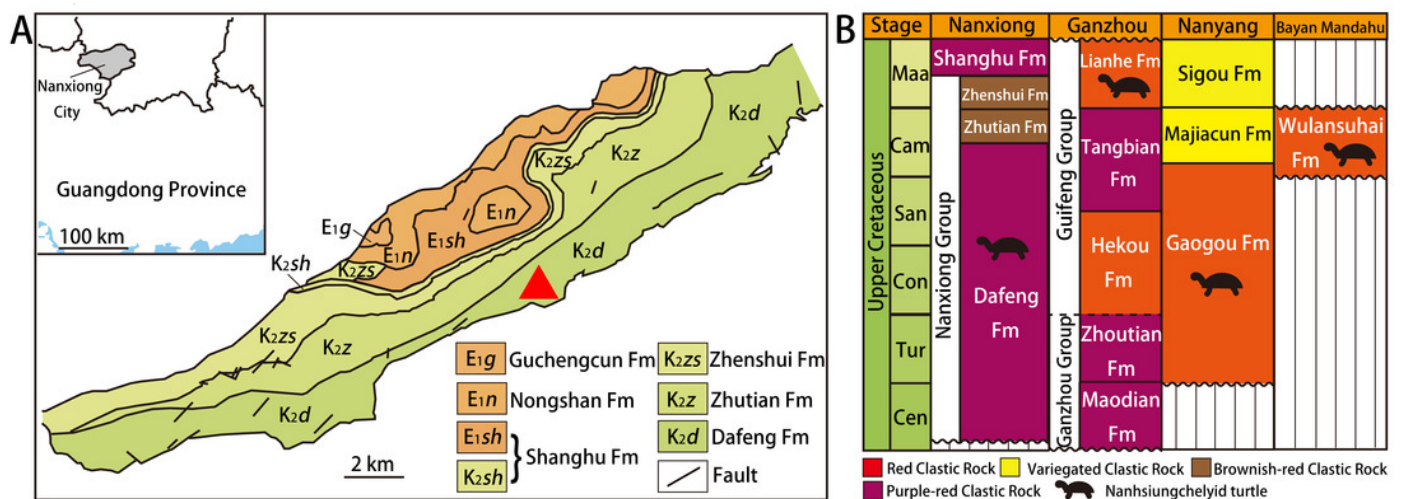


## Figure 2

Photograph (A) and outline drawing (B) of *Nanhsiungchelys yangi* (CUGW VH108) in anterior view.

Gray and black parts indicate the surrounding rock and openings of the skull, respectively. Scale bar equals 5 cm. Abbreviations: ca, carapace; md, mandible; pl, plastron; sk, skull.

A



B

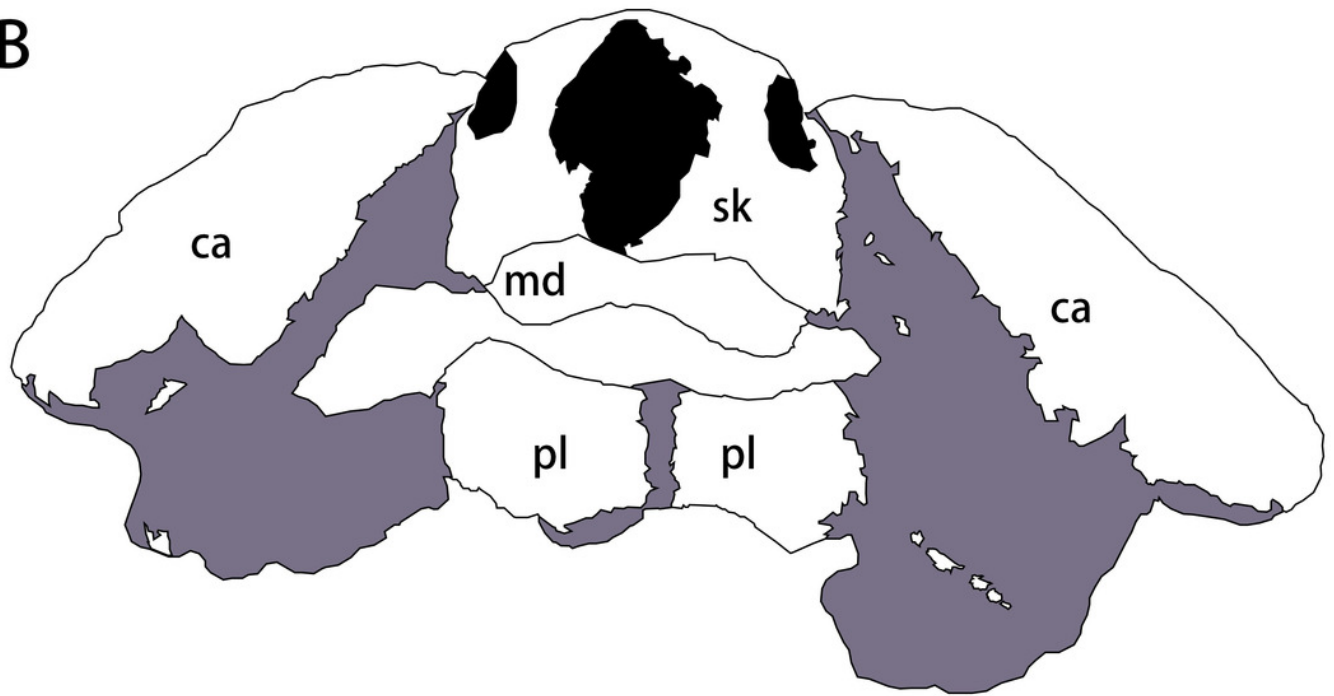


## Figure 3

The skull and carapace of *Nanhsiungchelys yangi* (CUGW VH108).

(A, B) Photograph and outline drawing of the skull and carapace in dorsal view, with a magnified view showing a distinct protrusion at the tip of anterolateral process (perpendicular to the surface of the carapace). (C, D) Photograph and outline drawing of the skull in left lateral view. (E, F) Photograph and outline drawing of the skull in right lateral view. Gray and black parts indicate the surrounding rock and openings of the skull, respectively. Scale bars equal 5 cm. Abbreviations: ca, carapace; fr, frontal; ju, jugal; md, mandible; mx, maxilla; pa, parietal; pf, prefrontal; pm, premaxilla; po, postorbital; qj, quadratojugal.

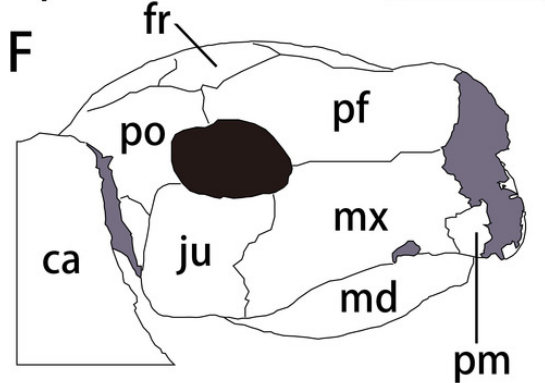
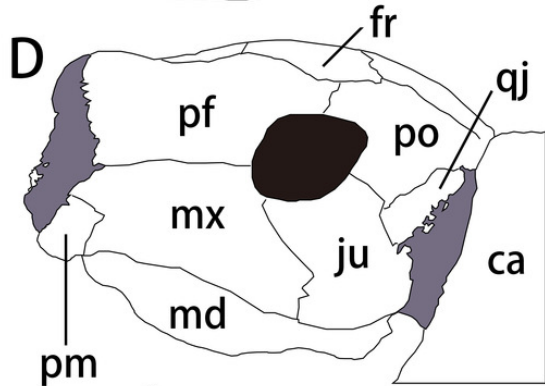
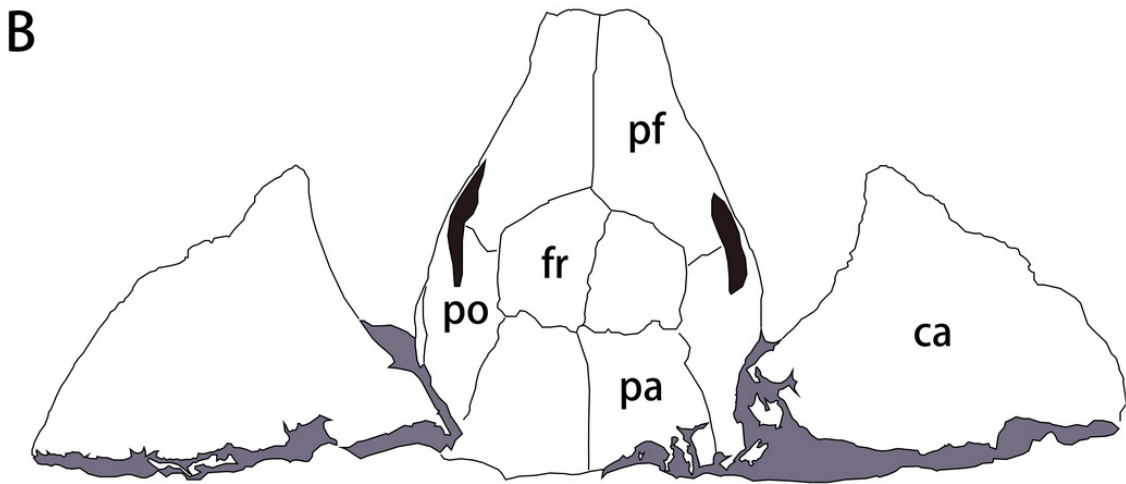
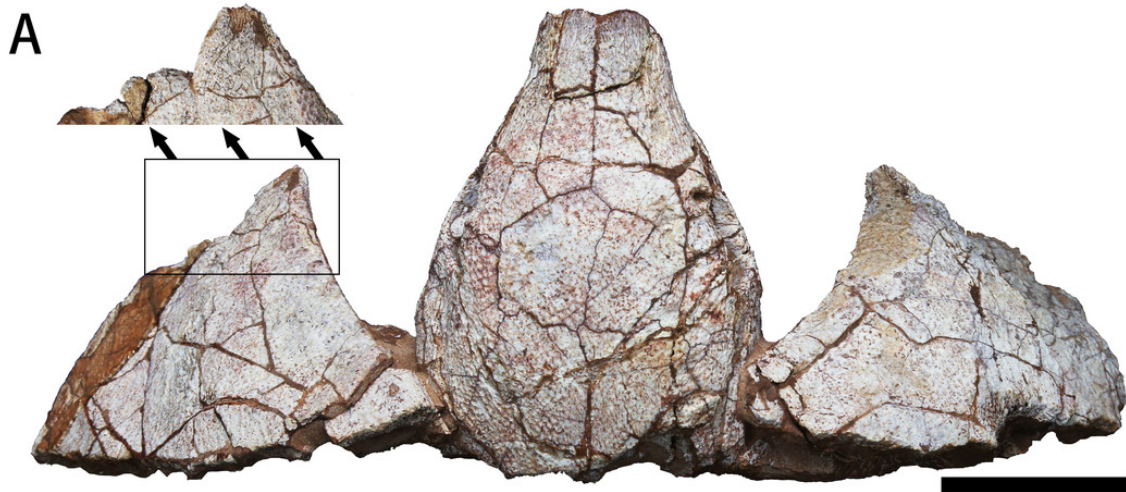


## Figure 4

Photograph (A) and outline drawing (B) of *Nanhsiungchelys yangi* (CUGW VH108) in ventral view.

Bold lines represent the sulci between scutes and gray parts indicate the surrounding rock. Scale bar equals 5 cm. Abbreviations: ca, carapace; epi, epiplastron; ent, entoplastron; Gu, gular scute; Hum, humeral scute; md, mandible; sk, skull.

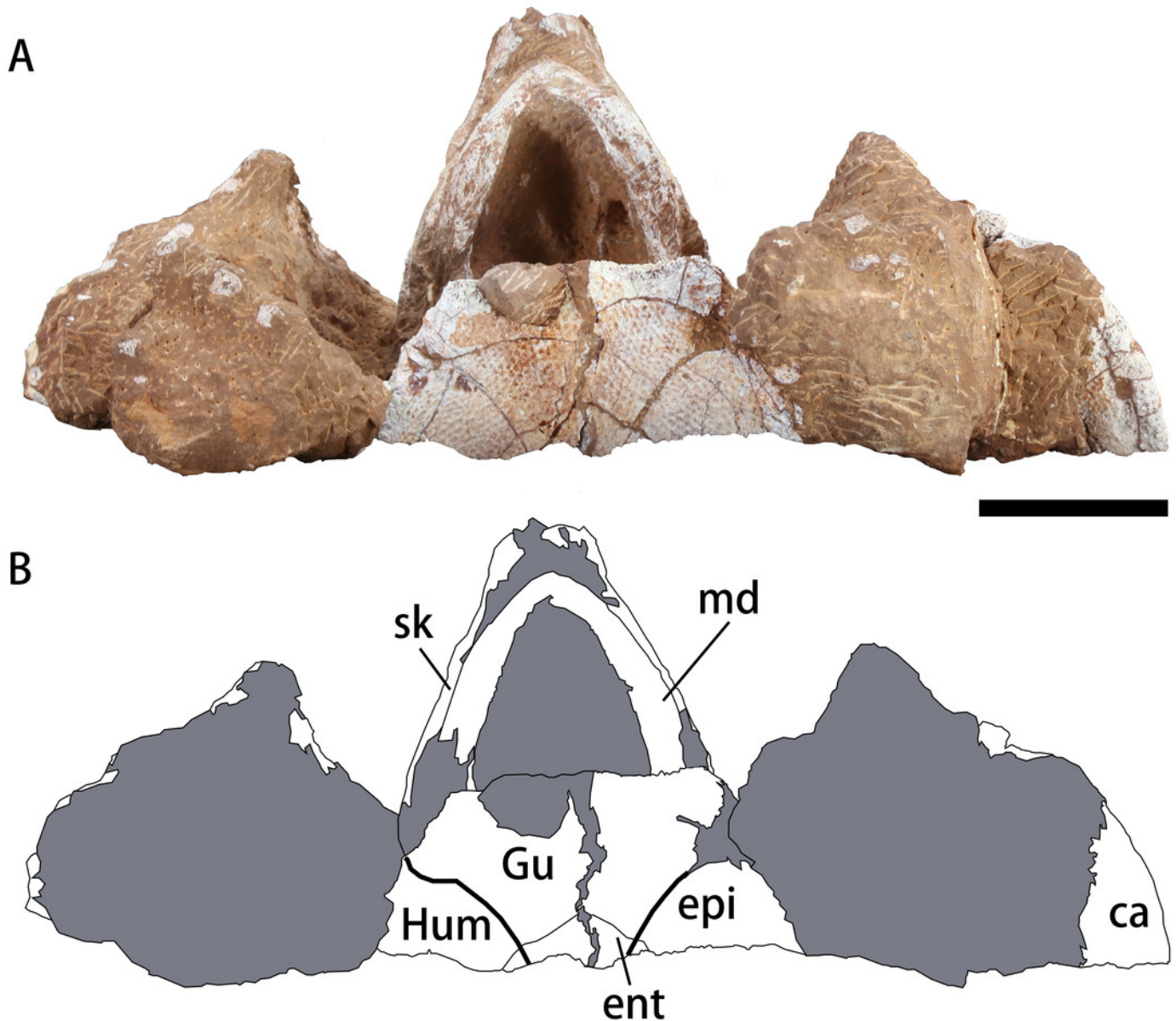


## Figure 5

Outline drawings of three nanhsiungchelyids.

(A) Skull and carapace of *Nanhsiungchelys wuchingensis*, after Tong & Li (2019) and Hirayama et al. (2001). (B) Carapace of *Anomalochelys angulata*, after Hirayama et al. (2001). (C) Skull and partial carapace of *Nanhsiungchelys yangi* (CUGW VH108). (D) Skull of *Nanhsiungchelys wuchingensis* in left lateral view, after Tong & Li (2019); arrows indicate the concave prefrontal. (E) Skull of *Nanhsiungchelys yangi* (CUGW VH108) in left lateral view. Scale bars equal 10 cm. Bold black lines represent the sulci between scutes, thin gray lines indicate the sutures between bones, and dashed lines indicate a reconstruction of poorly preserved areas. Abbreviations: bones: art, articular; Bif, bifurcation; co, costal; den, dentary; fr, frontal; ju, jugal; mx, maxilla; md, mandible; n, neural; nu, nuchal; p, peripheral; pa, parietal; pf, prefrontal; pm, premaxilla; po, postorbital; Pro, protrusion; qj, quadratojugal; sq, squamosal; scutes: M, marginal scute; P, pleural scute; V, vertebral scute; measurement: ECL, entire carapace length; MHW, maximum head width; SCW, straightline carapace width.

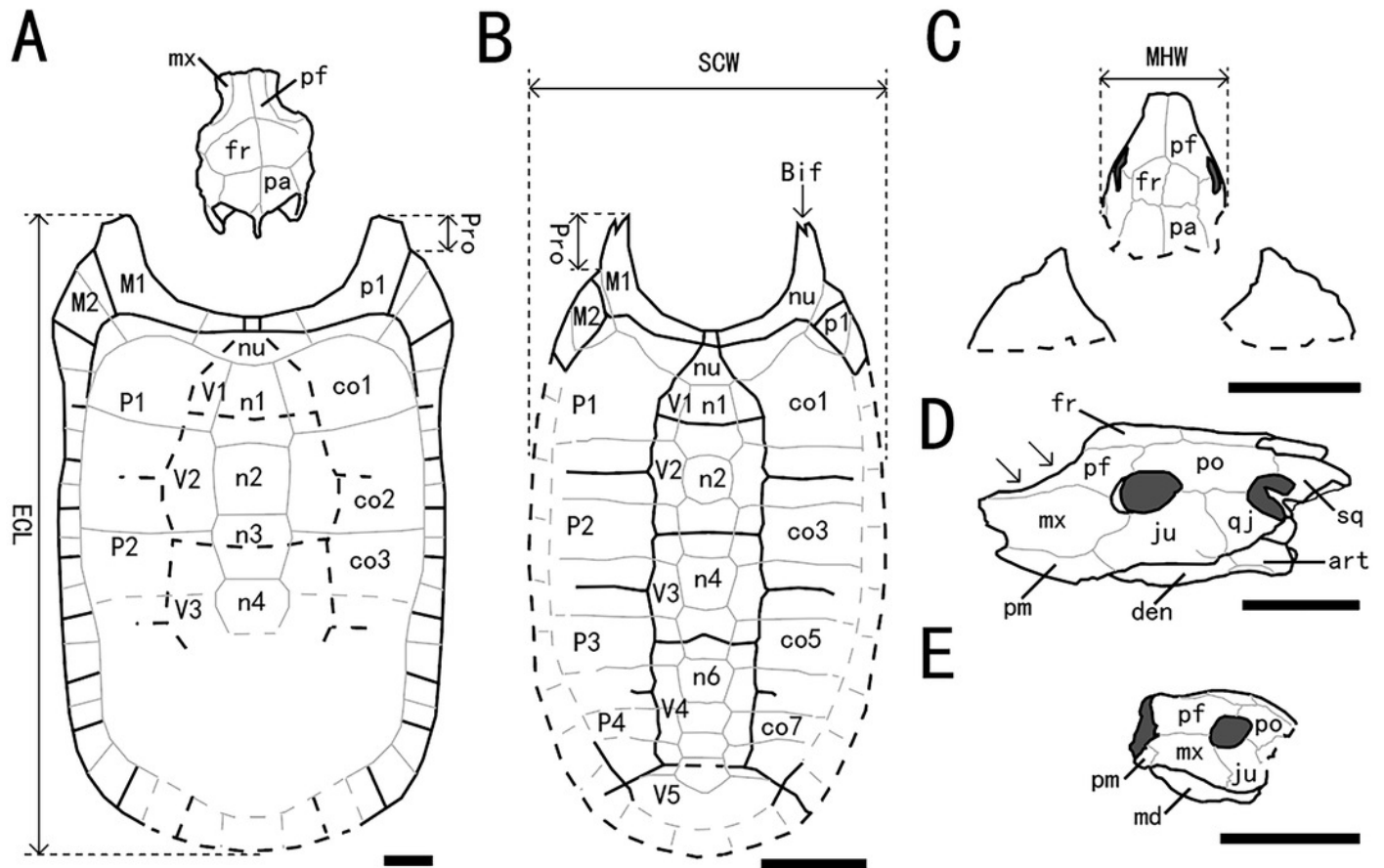


## Figure 6

Time-scaled strict consensus tree of Nanhsiungchelyidae.

Numbers above nodes are bootstrap support values and numbers below nodes are Bremer support values. Please note that the bootstrap support values less than 50 and the Bremer support values equal to 1 are not shown here. Temporal distributions of species based on Danilov et al. (2013), Li & Tong (2017), Syromyatnikova & Danilov (2009), Tong et al. (2016), Mallon & Brinkman (2018), and Xi et al. (2021). Abbreviations: Hau, Hauterivian; Barr, Barremian; Apt, Aptian; Alb, Albian; Cen, Cenomanian; Tur, Turonian; Con, Coniacian; San, Santonian; Cam, Campanian; Maa, Maastrichtian; Dan, Danian; Sel, Selandian; Tha, Thanetian; Ypr, Ypresian; Lut, Lutetian; Bar, Bartonian; Pri, Priabonian; Rup, Rupelian; Cha, Chattian; Aqu, Aquitanian; Bur, Burdigalian.

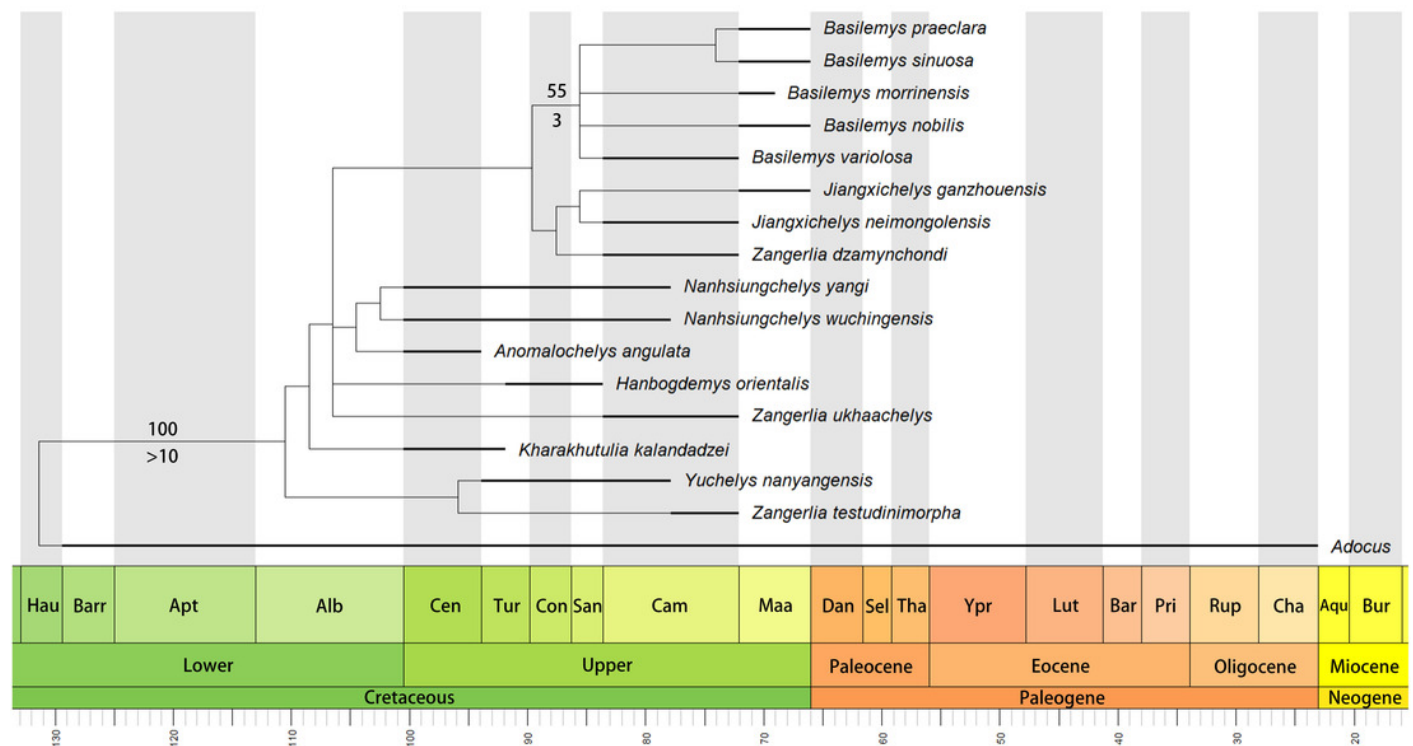


## Figure 7

3-D plots of streamlines at flow velocities of  $1.0 \text{ m s}^{-1}$ .

(A) and (B) are the model of *Nanhsiungchelys yangi* (in left lateral and dorsal views, respectively); (C) and (D) are the model of hypothetical turtle I (in left lateral and dorsal views, respectively), whose anterior carapace and body are blunt; (E) and (F) are the model of hypothetical turtle II (in left lateral and dorsal views, respectively), whose anterior carapace is streamlined and similar to most freshwater turtles. The arrows indicate the anterolateral processes. The direction of ambient flow is from left to right.

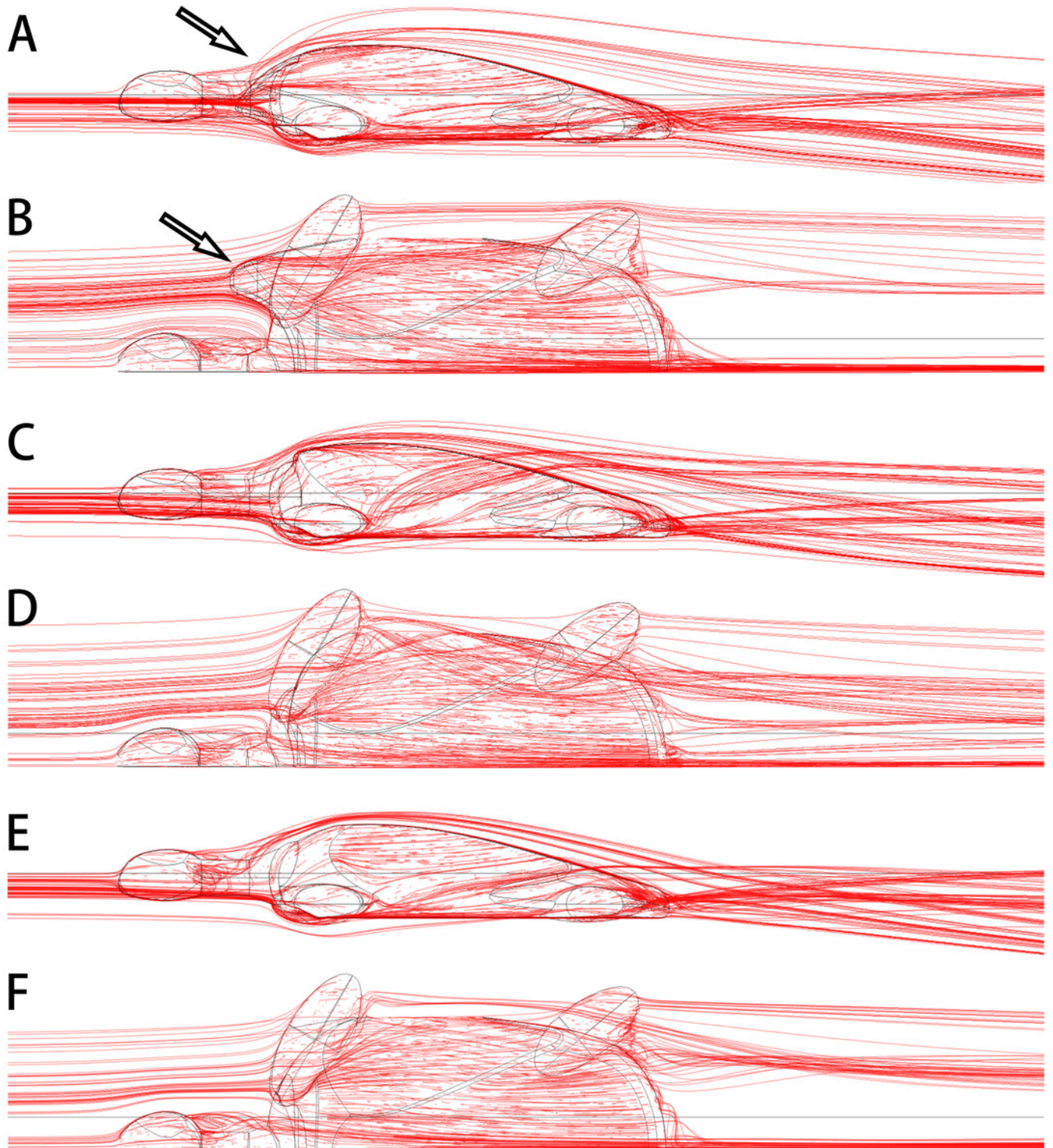


**Table 1** (on next page)

Taxonomy and distribution of Nanhsiungchelyidae in China

Note: this table does not include small fragments which has less taxonomic significance.

- 1 Table 1:  
2 Taxonomy and distribution of Nanhsiungchelyidae in China

Taxa	Specimen Number	Location	Age	Stratigraphic Unit	References
<i>Nanhsiungchelys wuchingensis</i>	IVPP V3106	Nanxiong, Guangdong	Late Cretaceous (Cenomanian–middle Campanian)	Dafeng Formation	<i>Yeh (1966)</i> <i>Tong &amp; Li (2019)</i>
<i>Nanhsiungchelys</i> sp.	SNHM 1558	Nanxiong, Guangdong	Late Cretaceous (Cenomanian–middle Maastrichtian)	Nanxiong Group	<i>Hirayama et al. (2009)</i> <i>Li &amp; Tong (2017)</i>
<i>Nanhsiungchelys yangi</i> sp. nov.	CUGW VH108	Nanxiong, Guangdong	Late Cretaceous (Cenomanian–middle Campanian)	Dafeng Formation	This paper
<i>Jiangxichelys neimongolensis</i>	IVPP RV96007, IVPP RV96008, IVPP 290690-6 RV 96009, IVPP 020790-4 RV 96010, IVPP 130790-1 RV 96011, IMM 4252, IMM 2802, IMM 96NMBY-I-14, IMM 93NMBY-2	Bayan Mandahu, Inner Mongolia	Late Cretaceous (Campanian)	Wulansuhai Formation	<i>Brinkman &amp; Peng (1996)</i> <i>Brinkman et al. (2015)</i> <i>Li &amp; Tong (2017)</i>
<i>Jiangxichelys ganzhouensis</i>	NHMG 010415, JXGZ(2012)-178, JXGZ(2012)-179, JXGZ(2012)-180, JXGZ(2012)-182	Ganzhou, Jiangxi	Late Cretaceous (Maastrichtian)	Lianhe Formation	<i>Tong &amp; Mo (2010)</i> <i>Tong et al. (2016)</i>
<i>Yuchelys nanyangensis</i>	HGM NR09-11-14, CUGW EH051	Nanyang, Henan	Late Cretaceous (Turonian–middle Campanian)	Gaogou Formation	<i>Tong et al. (2012)</i> <i>Ke et al. (2021)</i>
Nanhsiungchelyidae indet.	Specimen number was unknown. The authors named it as 'Hefei specimen'	Jiangxi	Late Cretaceous	Unknown	<i>Hu et al. (2016)</i>

- 3 Note: this table does not include small fragments which has less taxonomic significance.

4

**Table 2** (on next page)

Main differences among the three species of *Nanhsiungchelys*

## 1 Table 2:

2 Main differences among the three species of *Nanhsiungchelys*

Character	<i>Nanhsiungchelys yangi</i>	<i>N. wuchingensis</i>	<i>Nanhsiungchelys</i> sp. (SNHM 1558)
Snout	triangular (in dorsal view)	trumpet shaped	unknown
Premaxilla	higher than wide	wider than high in lateral view and has an inverse Y-shape in ventral view	unknown
Maxilla	unseen in dorsal views; a small portion of the maxilla extends posterior and ventral of the orbit	visible in dorsal views; the maxilla is located entirely anterior to the orbit	unknown
Jugal	higher than wide	wider than high	unknown
Prefrontal	convex dorsally behind the naris	concave behind the naris	unknown
Parietal	bigger than the frontal	smaller than the frontal	unknown
Mandible	the middle and posterior parts of the mandible are more robust than the most anterior part in ventral view	nearly all parts of the mandible are equal in width	unknown
Entoplastron	the angle between the two anterior edges of the entoplastron is wide (~110°)	the angle between the two anterior edges of the entoplastron is only ~100°	unknown
Anterolateral processes	wide	wide	slender

References	this paper	<i>Tong &amp; Li (2019)</i>	<i>Hirayama et al. (2009)</i>
------------	------------	-----------------------------	-------------------------------

3